Harmful Algae 93 (2020) 101773

Contents lists available at ScienceDirect

Harmful Algae

journal homepage: www.elsevier.com/locate/hal

Ecological time series and integrative taxonomy unveil seasonality and diversity of the toxic diatom *Pseudo-nitzschia* H. Peragallo in the northern Adriatic Sea

Timotej Turk Dermastia[a,d,*], Federica Cerino[b], David Stanković[a], Janja Francé[a], Andreja Ramšak[a], Magda Žnidarič Tušek[c], Alfred Beran[b], Vanessa Natali[b], Marina Cabrini[b], Patricija Mozetič[a]

[a] National Institute of Biology, Marine Biology Station Piran, Fornače 41, 6330 Piran, Slovenia
[b] Istituto Nazionale di Oceanografia e di Geofisica Sperimentale – OGS, via Piccard 54, 34151 Trieste, Italy
[c] National Institute of Biology, Department of Biotechnology and Systems Biology, Večna pot 111, 1000 Ljubljana, Slovenia
[d] International Postgraduate School Jožef Stefan, Jamova cesta 39, 1000 Ljubljana, Slovenia

ARTICLE INFO

Keywords:
Pseudo-nitzschia
Morphology
Phylogeny
Seasonality
Time series
Adriatic Sea

ABSTRACT

Pseudo-nitzschia H. Peragallo (1900) is a globally distributed genus of pennate diatoms that are important components of phytoplankton communities worldwide. Some members of the genus produce the neurotoxin domoic acid, so regular monitoring is in place. However, the identification of toxic members in routine samplings remains problematic. In this study, the diversity and seasonal occurrence of *Pseudo-nitzschia* species were investigated in the Gulf of Trieste, a shallow gulf in the northern Adriatic Sea. We used time series data from 2005 to 2018 to describe the seasonal and inter-annual occurrence of the genus in the area and its contribution to the phytoplankton community. On average, the genus accounted for about 15 % of total diatom abundance and peaked in spring and autumn, with occasional outbreaks during summer and large inter-annual fluctuations. Increased water temperature and decreased salinity positively affected the presence of some members of the genus, while strong effects could be masked by an unsuitable definition of the species complexes used for monitoring purposes. Therefore, combining morphological (TEM) and molecular analyses by sequencing the ITS, 28S and *rbcL* markers, eight species were identified from 83 isolated monoclonal strains: *P. calliantha*, *P. fraudulenta, P. delicatissima*, *P. galaxiae, P. mannii*, *P. multistriata, P. pungens* and *P. subfraudulenta*. A genetic comparison between the isolated strains and other strains in the Mediterranean was carried out and *rbcL* was inspected as a potential barcode marker in respect to our results. This is the first study in the Gulf of Trieste on *Pseudo-nitzschia* time series from a long-term ecological research (LTER) site coupled with molecular data. We show that meaningful ecological conclusions can be drawn by applying integrative methodology, as opposed to the approach that only considers species complexes. The results of this work will provide guidance for further monitoring efforts as well as research activities, including population genetics and genomics, associated with seasonal distribution and toxicity profiles.

1. Introduction

Pseudo-nitzschia diatoms are well-recognized and extensively studied components of phytoplankton communities worldwide. The genus comprises 54 described species (Bates et al., 2018; Huang et al., 2019), among which 26 are known to be toxic due to the production of domoic acid (DA), a potent neurotoxin, which can cause harmful effects on human health and marine organisms (Lelong et al., 2012; Trainer et al., 2012).

Precise determination of species identity using light microscopy (LM) is inadequate for most species. Therefore, morphological observations require the use of electron microscopy and even this might not reveal the entire complexity (Amato et al., 2007; Stern et al., 2018a). There are many cases of cryptic and pseudocryptic species within distinct clades and, therefore, genetic tools are used to overcome this problem (Lundholm et al., 2006; Amato et al., 2007; Lelong et al., 2012). Phylogenetic analysis for this genus is performed by analysing the sequence data of several phylogenetic markers. The most commonly

* Corresponding author.
E-mail address: timotej.turkdermastia@nib.si (T. Turk Dermastia).

https://doi.org/10.1016/j.hal.2020.101773
Received 3 July 2019; Received in revised form 6 January 2020; Accepted 3 February 2020
Available online 28 February 2020

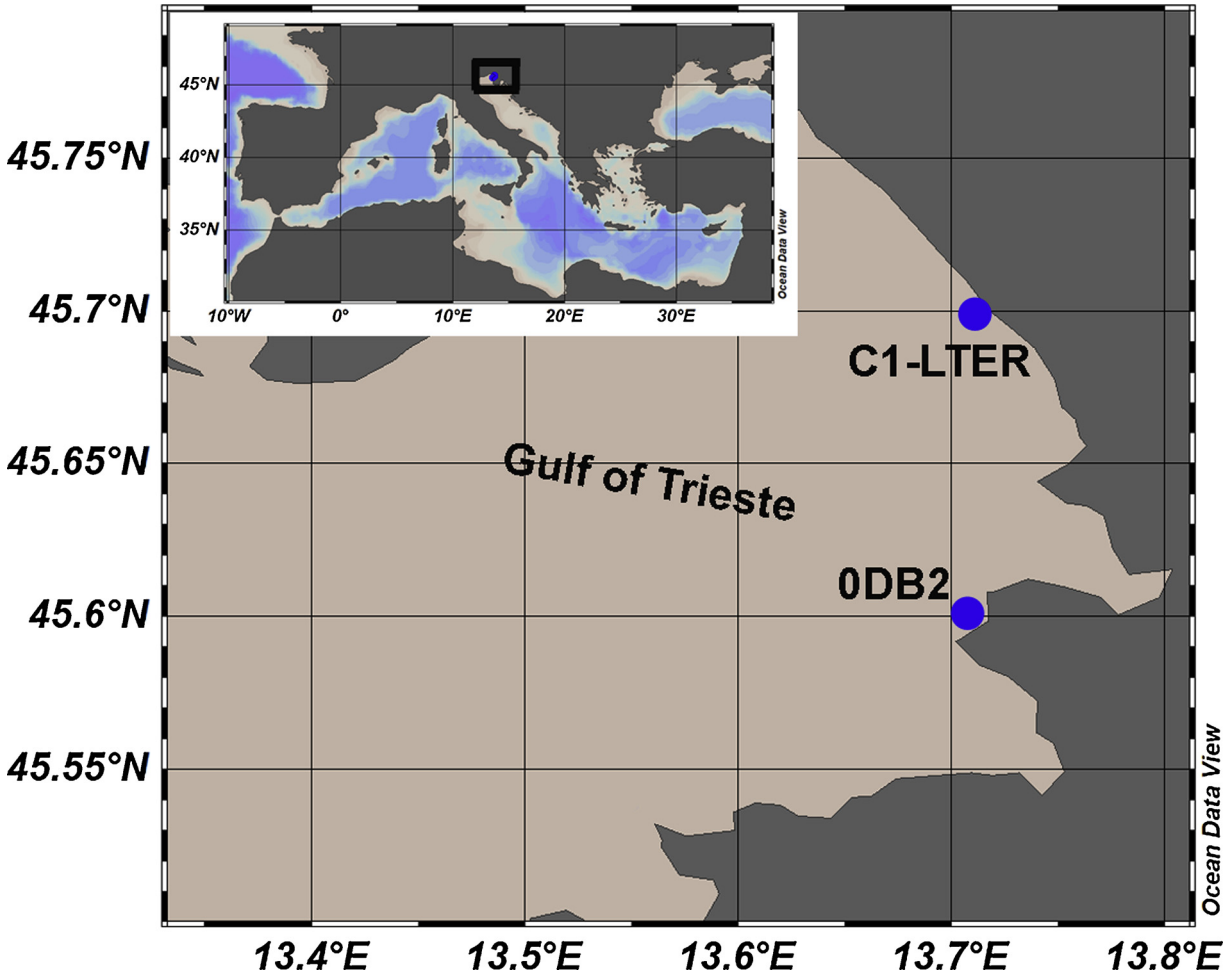

Fig. 1. Map of the study area in the northern Adriatic Sea (Mediterranean Sea) showing the location of the sampling stations (C1-LTER and 0DB2).

ones used are: the large ribosomal subunit gene (28S), internal transcribed spacer regions (ITS), plastid encoded genes such as the RuBiSCo large subunit (*rbcL)* (e.g. Amato et al., 2007) and mitochondrial encoded *cox1* (Lim et al., 2018). Three large clades have been identified (reviewed in Trainer et al., 2012): *P. seriata*, *P. delicatissima* and *P. pseudodelicatissima*. While the *P. seriata* group is well-resolved, the *P. delicatissima* and *P. pseudodelicatissima* complexes host a large number of cryptic species with new species continuously being described (Bates et al., 2018). In total, 12 new species and one variety have been described since 2012 in the *P. pseudodelicatissima* complex and two new species in the *P. delicatissima* complex (Bates et al., 2018, and references therein; Huang et al., 2019). Integrative taxonomy has proved key in distinguishing species complexes into distinct entities while building the capacity for researchers to gain a better understanding of their studied ecosystems (Orive et al., 2010; Lundholm et al., 2012; Ajani et al., 2013; Huang et al., 2019). This is the first step when threates such as harmful algal blooms (HABs) need to be managed correctly or even forecasted (Fehling et al., 2006; Lane et al., 2009; Anderson et al., 2010; Mccabe et al., 2016). Forecasts usually deal with genus or species complex data at best, since this is usally the only long-term data available and is derived from LM counts or automatic samplers (Anderson, 2014). Like-wise, ecological studies from which models are built rely primarily on LM, although novel molecular techniques are constantly being incorporated into long-term ecological research (LTER) management giving us more insight into the complex world of plankton (Stern et al., 2018b; Zingone et al., 2019). By incorporating knowledge and data from detailed morphological and molecular analyses of locally isolated strains into LTER series, valuable information can be obtained thus rendering the LTER stations more functional (a). Thus, LM data alone, cannot reveal potential threats due to toxic species outbreaks and may miss novel species that show up in regular samplings. Moreover, taxonomists and LTER operators commonly face the lack of prior knowledge due to the incompleteness of curated public and local reference databases. Indeed, in the advent of high-throughput sequencing techniques that are being incorporated into LTER strategies the knowledge of local protist molecular diversity is crucial for the correct and robust clustering of reads (Stern et al., 2018a).

No comprehensive integrated approach combining morphological transmission electron microscopy (TEM) examination and molecular analyses extending over a longer time period has been published so far for the Adriatic, and limited sequence data exist for the area. Existing reports on species diversity and composition rely on TEM data at best (Caroppo et al., 2005; Ljubešić et al., 2011; Marić et al., 2011; Arapov et al., 2016, 2017), while only two studies include genetic data but only for few species (Penna et al., 2013; Pugliese et al., 2017). In this respect, the northernmost region of the Adriatic Sea, the Gulf of Trieste (GoT) has hardly been studied and the true diversity of the genus remains unknown despite decade-long surveys of the phytoplankton community structure in the GoT. Considering the fact that the Gulf is an important fishing and aquaculture area, particularly for mussel farms (Solidoro et al., 2010), which applies to many Adriatic coastal areas, it is essential to assess and identify harmful algal species that can influence these activities. Until now, strains of only two species from the Adriatic have been found to produce DA in cultures, *P. delicatissima* (Penna et al., 2013) and *P. multistriata* (Pistocchi et al., 2012), albeit at very low concentrations. Monitoring schemes at aquaculture sites along the

eastern coast of the Adriatic Sea report on the occasional presence of DA in shellfish (Ujević et al., 2010; Ljubešić et al., 2011) and phytoplankton net samples (Arapov et al., 2016) during *Pseudo-nitzschia* blooms. However, shellfish toxicity was always below the regulatory limit (20 mg kg^{-1}; Regulation (EC) 853 of 2004) and the causative agent of toxicity was not identified.

The main aims of this study were to unveil the diversity of the potentially toxic *Pseudo-nitzschia* species in the GoT (Adriatic Sea), by combining morphological analysis and molecular methods over a 2-year study period, and to describe the seasonal occurrence of species or groups in a 14-year long time series. We also wanted to see how this data could be coupled and utilised for LTER management and assessment of the ecological status. Finally, we wanted to re-evaluate the utility of the *rbcL* marker as a potential diatom barcode, proposed recently (Rimet et al., 2016).

2. Methods

2.1. Study area

The GoT is a shallow coastal area (maximum depth of about 25 m) at the northernmost end of the Adriatic Sea (Fig. 1). Its oceanographic properties are affected by water mass exchanges with the northern Adriatic at the open western boundary, local meteorological conditions that induce a pronounced seasonal seawater temperature cycle (from winter minima of 5 °C to summer maxima > 26 °C) and by several freshwater inputs along the northern and southern coastline (Malačič et al., 2006; Cozzi et al., 2012). The Isonzo River is the major source of freshwater and allochthonous nutrients in the GoT, and deeply influences the hydrology, biogeochemistry and productivity of this coastal area (Cozzi et al., 2012). The combination of atmospheric heating of the surface layer and increased freshwater inflow during spring, establishes a pycnocline, which intensifies during summer, while in winter the water column is well-mixed (Malačič, 1991). All these features are ultimately reflected in strong seasonal and inter-annual variability in ecosystem structure and functioning, which primarily includes changes in plankton communities and primary production (Mozetič et al., 1998; Fonda Umani et al., 2007; Talaber et al., 2018).

2.2. Cell isolation and cultivation

In the Slovenian part of the GoT, phytoplankton samples for isolation and cultivation were collected monthly from October 2016 to March 2018 with some additional sampling events in 2019. Five vertical and five horizontal hauls were performed at the 0DB2 station (13°42′20″ E and 45°35′57″ N, bottom depth 17 m) next to a mussel farm (Fig. 1).

Samples were stored in a darkened glass container and immediately returned to the laboratory where single cell isolations were performed by selecting *Pseudo-nitzschia* cells and washing them repeatedly in 0.22 µm filtered seawater until no other phytoplankton species were visibly present. This process was performed using drawn Pasteur pipettes under light microscopy at 100x magnification. Isolated cells were first grown in 3 × 4 Nunclon® culture plates containing 1/5x L1 medium. After two weeks, the plates were checked for growing cells that were subsequently transferred to autoclaved 50 ml Erlenmayer flasks containing L1 medium. These flasks were kept at 20 °C on a 12/12 light cycle for growth and subsequent analysis. The cultures were transferred to fresh medium every two weeks.

In the Italian part of the GoT, samples were collected in October 2016 by a vertical haul at the Long-Term Ecological Research station, C1-LTER (45°42′2.99″ N and 13°42′36.00″ E, bottom depth 17.5 m), located 270 m off the coast (http://nettuno.ogs.trieste.it/ilter/BIO/history.html). Single *Pseudo-nitzschia* cells were isolated by micropipetting and maintained as described before.

2.3. Light and transmission electron microscopy

Cells were measured and photographed using a light microscope (Zeiss Axio Observer.Z1 and LeicaDM2500, Germany) equipped with a digital camera (AxioCam MRc5 and Leica DFC490, Germany).

For TEM observations where only the silicate frustule is observed, cultures were cleaned and prepared using nitric and sulphuric acid to remove organic matter, as described in the Assemble protocol of Percopo and Sarno (https://www.assemblemarine.org/assets/Uploads/Documents/tool-box/Diatom-Cleaning-with-Nitric-Sulfuric-Acids.pdf). Briefly, 10 mL of culture was centrifuged for 10 min at 2500 rpm in a glass centrifuge tube, the supernatant was removed and the pellet resuspended in acid at a ratio of 1:1:4 (sample: 65 % HNO_3: 98 % H_2SO_4). The mixture was placed over a propane flame until it started to boil and the plume turned white/colourless. The mixture was then left to cool down and was serially diluted with MilliQ water followed by centrifugation to remove the residual acid. The prepared samples were subsequently stored at room temperature. A drop of the cleaned material was placed on Formvar-coated copper grids (SPI supplies® 75, 100 and 400 mesh), left to dry overnight and observed using transmission electron microscopy (Philips CM 100 equipped with a Bisocan CCD camera and Olympus Quemesa iTEMon FEI EM208).

2.4. DNA extraction, PCR amplification and sequencing

DNA was extracted from cultures in the exponential growth phase, which was established by counting cells in a Fuchs-Rosenthal counting chamber on successive days. The E.Z.N.A. Mollusc DNA (Omega Biotek) and Quick-DNA™ Fungal/Bacterial Miniprep (Zymo Research) kits were used for the extraction process. Different culture volumes (10 − 50 mL) were centrifuged and the pellet was homogenized using a sterilized hand-held portable homogenizer. The material was then resuspended in the provided buffer with proteinase K. Subsequent steps in DNA extraction followed the producer's guidelines. Polymerase chain reaction (PCR) was performed with a series of primers targeting three gene fragments; namely, the entire transcribed spacer region of the nuclear rDNA (ITS1/5.8S/ITS2), here on ITS, the large ribosomal subunit (28S) gene and the gene encoding the large subunit of the ribulose-1.5-biphosphate carboxylase/oxidase protein (*rbcL*). PCR amplification was performed by a recombinant *Taq DNA* polymerase (Thermo-Fisher Scientific) or TopTaq polymerase (Qiagen) in a total volume of 25 µL. The PCR protocols for the respective gene markers and the

Table 1
PCR protocols and primers.

Enzyme	Marker	Primer set	Primer reference	Protocol				
TF Taq	ITS1-2	ITS1/ITS4	White et al., 1990	1:94 °C 5 min	2: 94 °C 45 s	3: 52 °C 30 s	4: 72 °C 90 s [2–4 35x]	5:72 °C 8min
TF Taq	28S	D1R-F/D3B-R	Nunn et al., 1996 Scholin et al., 1994	1:94 °C 5 min	2: 94 °C 45 s	3: 52 °C 30 s	4: 72 °C 90 s [2–4 35x]	5:72 °C 8min
TopTaq	ITS1-2	ITS-F/ITS-R	Murray et al., 2012	1:94 °C 3 min	2: 94 °C 30 s	3: 52 °C 30 s	4: 72 °C 60 s [2–4 35x]	5:72 °C 10min
TopTaq	28S	D1R-F/D3B-R	Scholin et al., 1994 Nunn et al., 1996	1:94 °C 5 min	2: 94 °C 45 s	3: 52 °C 30 s	4: 72 °C 60 s [2–4 35x]	5:72 °C 10min
TopTaq	*rbcL*	DP_rbcl1/7	Jones et al., 2005	1:94 °C 5 min	2: 94 °C 45 s	3: 52 °C 30 s	4: 72 °C 90 s [2–4 35x]	5:72 °C 10min

corresponding primers that were used are presented in Table 1. In addition, internal primers l1F and l1R were used for sequencing the *rbcL* region for some problematic amplicons (Amato et al., 2007). Sanger sequencing was carried out by *Macrogen Inc.,* using the same primers as for previous amplification (Table 1). Chromatograms were quality checked and assembled in *Chromas Pro (v.2.1.8.)*. The identity of sequences was confirmed with BLASTn service.

2.5. Phylogenetic analysis

All available sequences of *Pseudo-nitzschia* species from the GenBank database were aligned with our sequences and included in the final dataset. Sequences were aligned using *MAFFT 7* (Katoh and Standley, 2013), applying different strategies depending on the marker. 28S and *rbcL* sequences were aligned using the G-INS-1 progressive method, while both the G-INS-1 progressive method and the FFT-NS-I iterative method were tested for ITS.

Gene markers (ITS2, 28S and *rbcL*) were analysed separately in order to obtain distinct phylogenies.The ITS2 alignment was 260bp, while phylogenies of 28S and *rbcL* were constructed using 769bp and 1220bp alignments, respectively. The best evolutionary models were selected for each marker in *jModelTest* (Posada, 2008). The selected model was used for Bayesian inference of phylogenies, using MrBayes v.3.2.6 (Ronquist et al., 2012). For each marker, the analysis was run for 5.000.000 generations in 4 parallel chains and until the average standard deviation had fallen below 0.01. Chain diagnostics were performed in Tracer (v. 1.7.1.; Rambaut et al., 2018) where the estimated sample size (ESS) was confirmed to be above 700 for the LnL parameter and well above 1000 for all other parameters that are estimated in the Markov chain. An additional 312bp-long alignment of *rbcL* sequences was performed and phylogeny reconstructed to compare the species and strain recovery of the proposed *rbcL* diatom barcode (Rimet et al., 2016; Vasselon et al., 2017). Pairwise distances were calculated with MEGA7 (Kumar et al., 2016).

A TCS network (Templeton et al., 1992; Clement et al., 2000) was constructed using the PopArt software package (Leigh and Bryant, 2015) in order to obtain an insight into haplotype differentiation between different *Pseudo-nitzschia* species and strains found in the Adriatic and elsewhere in the Mediterranean Sea. The TCS network was constructed using sequences from the ITS2 and *rbcL* region. For the ITS2 network, we geotagged the sequences according to whether they were found in the GoT (on the Italian and Slovenian side separately), the north-west Adriatic (Pesaro) (Penna et al., 2013; Pugliese et al., 2017), Tyrrhenian Sea (Gulf of Naples, GoN) (several publications), NE Mediterranean (Greek coastal waters) (Moschandreou et al., 2012), NW Mediterranean (Catalan Coast) (Quijano-Scheggia et al., 2008b, 2009), and sequences belonging to strains outside the Mediterranean. Because of the highly divergent nature of ITS2, the alignment used in the phylogenetic tree reconstruction was selected for the most conserved sites using least stringent conditions defined in GBlocks (Castresana, 2000), to counteract alignment issues that create masked sites in parsimony networks. Likewise, *rbcL* sequences were geotagged into GoT (Italian and Slovenian side), GoN (Amato et al., 2007; D'Alelio and Ruggiero, 2015), the NW Mediterranean (Elandaloussi et al., unpubl.), and sequences belonging to strains outside the Mediterranean. The geographic location of the sequence was obtained from the location identifier in GenBank where possible.

2.6. Environmental characterization and phytoplankton analysis

To describe the typical seasonal cycle and inter-annual variability of *Pseudo-nitzschia* in the GoT, an 14-year long time-series of *Pseudo-nitzschia* grouped into two complexes, i.e. *seriata* and *delicatissima* complex, was considered. Samples were collected monthly from 2005 to 2018 at station C1-LTER (Fig. 1) for both environmental and phytoplankton data. In addition, phytoplankton counts of the two *Pseudo-nitzschia* complexes were also performed on seawater samples collected at station 0DB2 (period 2016–2019) and designated for species isolation and cultivation (see 2.2).

CTD temperature and salinity profiles were obtained with Idronaut Ocean Seven (models 401 and 316) and a SBE 19plus SEACAT multiparametric probes. Discrete seawater samples were collected with 5-L Niskin bottles at four depths (0.5, 5, 10, 15 m). Dissolved inorganic nutrient concentrations were determined colorimetrically on filtered samples with a Bran + Luebbe Autoanalyzer 3, up to December 2013, and afterwards with a QuAAtro (Seal Analytical), according to Hansen and Koroleff (1999).

For phytoplankton analysis, the samples were fixed with prefiltered and neutralized formaldehyde (1.6 % final concentration) (Throndsen, 1978). A variable volume of seawater (10 − 50 ml) was settled in an Utermöhl chamber depending on cell abundance (Utermöhl, 1958; Zingone et al., 2010). Cells (minimum 200) were counted along transects (1–2) at 400x magnification using inverted microscopes. Additionally, half of the sedimentation chamber was also examined at 200x magnification for more precise identification of less abundant microphytoplankton (> 20 μm) taxa. Species belonging to the *Pseudo-nitzschia* genus were separated into the two complexes distinguished in LM basing, according to cell width: *P.* spp. *delicatissima* complex (cell width < 3 μm) and *P.* spp. *seriata* complex (cell width > 3 μm). Additionally, *P. multistriata* and *P. pungens* were identified based on the sigmoid shape of the cell in girdle view and the visibility of striae, respectively. At C1-LTER, *P.* cf. *galaxiae* was also identified based on thin cell rostrata, while at 0DB2, *P.* cf. *fraudulenta* (composed of *P. fraudulenta* and *P. subfraudulenta*) was identified based on valve dimensions.

2.7. Statistical analysis

A non-parametric Spearman rank order correlation was used to assess the relationship among oceanographic parameters and abundance of *Pseudo-nitzschia* complexes. Analysis of Similarity (one-way ANOSIM) was carried out (1000 permutations) to test the significance of similarities in biological features among seasons and years.

Principal Component Analysis (PCA) was performed on a Euclidean distance matrix of selected normalized physical and chemical variables (temperature, salinity and dissolved inorganic nutrients) to characterize and differentiate the seasons. The centroids of the observations of each month were calculated and plotted against the PC1 *vs.* PC2 combination because they expressed most of the variance of the dataset. Furthermore, the log(X + 1) transformed abundances of *Pseudo-nitzschia* taxa identified with LM were fitted as supplementary variables (vectors) onto the ordination space.

We also conducted a non-metric multidimensional scaling analysis (NMDS) with species abundance data to further inspect potential seasonal patterns and the ordination of species complexes versus specific species in multidimensional space.

All these analyses were performed using the PRIMER software package (v.7).

Finally, the data from 0DB2, where isolations took place, was used in a proof-of-concept constrained correspondence analysis (CCA) to demonstrate how feeding molecular data into LTER management can improve research and monitoring. The methodological procedure for this is included in the supplementary data (S4).

The CCA of isolation-currated data was perfomed using R Statistical Software (R Core Team, 2019) and the "Vegan" package (Oksanen et al., 2019).

3. Results

3.1. Seasonal cycle and inter-annual variability of environmental properties, phytoplankton community and the Pseudo-nitzschia genus

The C1-LTER coastal station was characterized by a strong seasonal

cycle with cold winters (9.20 ± 1.44 °C, on average) and warm summers (22.62 ± 2.17 °C, on average) (S1: A). The highest temperature (28.34 °C) of the time series was measured in July 2015. Surface salinity drops that were registered during certain periods of almost each year indicate freshwater inputs of riverine and/or atmospheric origin (S1: B). The most evident and long-lasting persistence of a cooler subsurface water layer was observed in 2010.

Dissolved inorganic nitrogen (DIN) concentrations, calculated as the sum of ammonium, nitrite and nitrate concentrations, displayed higher values in autumn and winter with increases in spring in some years (S1: C). Elevated concentrations of DIN in the surface layer were particularly evident in years 2009, 2010, 2013 and 2014. Phosphate concentrations showed interannual variability but not a clear seasonality; on average, higher values were recorded in late autumn-early winter and in August (S1: D). Finally, silicate concentrations were generally higher in summer and winter in the deeper part of the water column, while surface peaks were measured in the spring of certain years (S1: E).

Considering the 14-year long phytoplankton time series (2005–2018) of the C1-LTER station, in terms of relative abundance, about 31 % of phytoplankton were represented by diatoms, and *Pseudo-nitzschia* spp. accounted for about 15 % of total diatoms averaged across all samples (Fig. 2). *Pseudo-nitzschia* species were generally present all year round with pronounced autumn blooms occurring annually and reaching 70–80 % of total phytoplankton community abundance. Autumn blooms were characterized by both the *delicatissima* and *seriata* complexes, while occasional spring blooms were due to the *delicatissima* complex (Fig. 3). The *P. delicatissima* complex was the main contributor to the total abundance of the genus, with cell numbers reaching 2.3 × 10^6 cells L^{-1}, while the *P. seriata* complex showed much lower abundances, rarely exceeding 10^4 cells L^{-1}. There was one extreme event, however, in April 2011 when the *P. seriata* complex reached 1.4 × 10^6 cells L^{-1} (Fig. 3C). The abundances of both complexes fluctuated at the inter-annual scale; however, these changes did not appear significant in the ANOSIM analysis. The ANOSIM analysis did not show any overall significant difference between years and seasons, except for some years that differed significantly from the others (R = 0.11, p = 0.01 and R = 0.051, p = 0.01, respectively).

To summarize the observations from the ecological time series, a PCA was performed. The ordination of samples is largely forced by temperature and salinity that shape PC2 (Fig. 4). The structuring of the complexes demonstrates the seasonal preference of the *seriata* complex for the winter/autumn period and the *delicatissima* complex for the spring/summer period. The latter is also evidenced by the statistically significant although weak correlation coefficient (ρ = 0.197, Table 2). A statistically significant correlation was also found between salinity and the *seriata* complex, while the whole genus was negatively correlated with silicate and inorganic nitrogen species. The PCA was coupled with data on *P. multistriata, P. pungens and P. galaxiae.* The structuring

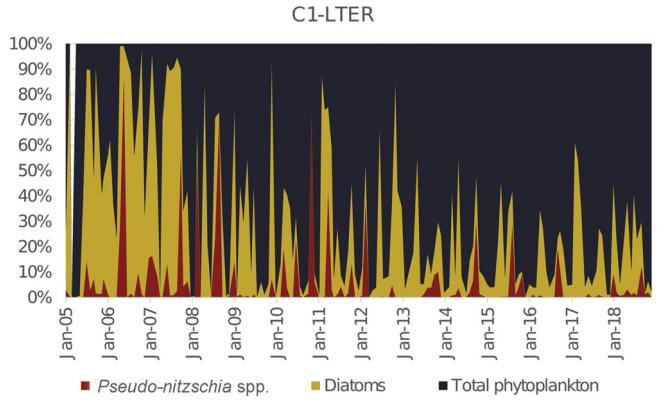

Fig. 2. Percentage abundances of *Pseudo-nitzschia* spp., diatoms and total phytoplankton from 2005 to 2018 at the station C1-LTER in the Gulf of Trieste.

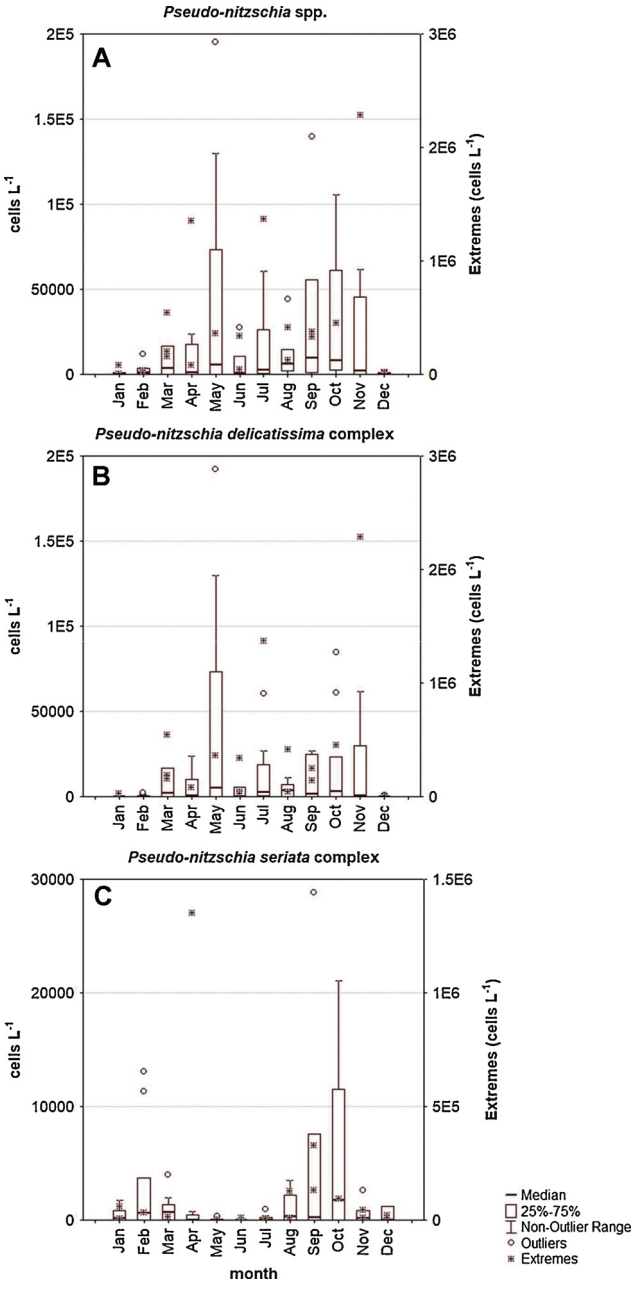

Fig. 3. Seasonal cycle of *Pseudo-nitzschia* spp. (A), *P. delicatissima* complex (B) and *P. seriata* complex (C) at the C1-LTER station in the Gulf of Trieste from 2005 to 2018. In the box plot of cell abundances, the bold line represents the median, the box the 25th and 75th percentiles of the distribution, the whisker the non-outlier range, the circle the outliers and the stars the extremes.

of *P. multistriata* into even more pronounced winter conditions is self-explanatory but this analysis shows that when reliable single-species data are considered the structure is more apparent than when the species are grouped into complexes that are often phylogenetically and ecologically incorrect, as will be demonstrated in the following section.

3.2. Diversity of the genus Pseudo-nitzschia in the GoT

Eight species of *Pseudo-nitzschia* were identified from 83 monoclonal strains isolated in the GoT (69 in Slovenian and 16 in Italian waters). Table 3 presents the species that have been identified along with the corresponding identification method and the number of strains within the respective species that have been sequenced or examined with TEM.

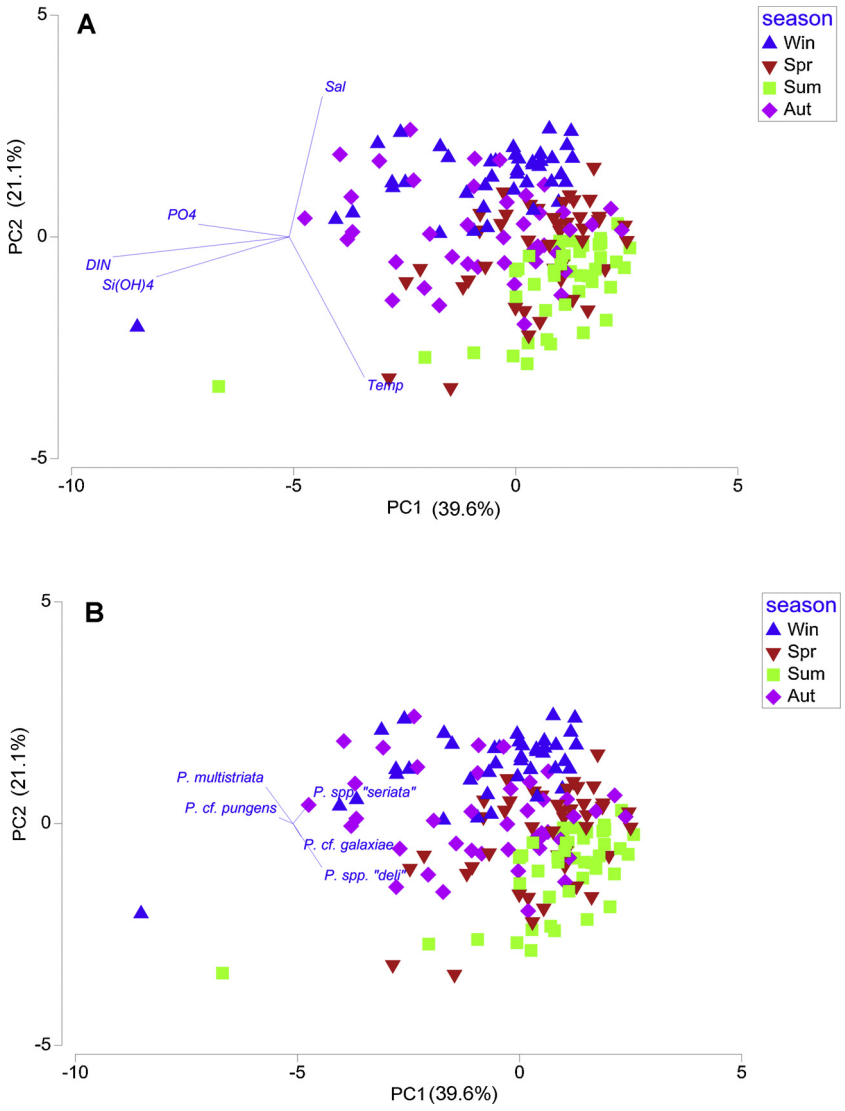

Fig. 4. Principal Component Analysis (PCA) ordination diagram of the selected variables (A). Symbols represent the centroids of the observations in each month. In B, the biological variables are fitted as supplementary variables. Temp: temperature; Sal: salinity; DIN: dissolved inorganic nitrogen; PO4: phosphate; Si(OH)4: silicate.

Accession numbers of sequenced strains are provided in Supplementary Table 1.

The autumn blooms of the *P. delicatissima* complex were characterized by isolates of *P. calliantha* and *P. mannii*, while the spring blooms of cells assigned to the *P. delicatissima* complex were characterized by isolates belonging to *P. delicatissima*. *P. galaxiae* cells were isolated only in August and September; nevertheless, LM identified cells that could have belonged to these species were also observed in the spring months. The *seriata* complex was more abundant in late autumn, winter and early spring. Of the species belonging to this complex, *P. multistriata* was isolated only in December and January, *P. subfraudulenta* in October and December, *P. fraudulenta* only in February, and *P. pungens* in December and March. The only species that was isolated in all seasons was *P. calliantha*. The species are described below and their morphometric data are summarized in Table 4. We also provide species-complex fluctuation data overlayed with species

Table 2
Spearman rank correlations among the water column integrated abundances of *Pseudo-nitzschia* taxa with environmental variables at the C1-LTER station for the period 2005–2018.

	Temperature	Salinity	PO_4	$Si(OH)_4$	DIN	NO_2+NO_3	*P. delicatissima* complex	*P. seriata* complex	*Pseudo-nitzschia* spp.
Temperature	1								
Salinity	**−0.424*****	1							
PO_4	−0.105	0.045	1						
$Si(OH)_4$	−0.105	−0.125	**0.296*****	1					
DIN	**−0.374*****	**−0.234****	**0.338*****	**0.535*****	1				
NO_2+NO_3	**−0.533*****	**−0.152***	**0.244****	**0.481*****	**0.913*****	1			
P. delicatissima complex	**0.197***	**−0.187***	**−0.157***	−0.047	−0.095	−0.088	1		
P. seriata complex	−0.059	**0.202****	−0.036	−0.116	−0.010	0.004	0.063	1	
Pseudo-nitzschia spp.	**0.199****	−0.079	−0.095	**−0.189***	**−0.172***	**−0.159***	**0.766*****	**0.508*****	1

Table 3
List of species identified in the Gulf of Trieste with information about the number of strains isolated for each species, isolation site and season (I: Italy; S: Slovenian; W: winter; SP: spring; SU: summer; A: autumn), observation methods (LM: light microscopy; TEM: transmission electron microscopy) and sequenced genes (28S, ITS, *rbcL*). For full strain summary see Supplementary Table 1.

Species	Strain number	Location	Season isolated	Methods
P. calliantha	21	I,S	SP,SU,A,W	LM,TEM,ITS,28S,*rbcL*
P. delicatissima	20	S	SP	LM,TEM,ITS,28S,*rbcL*
P. fraudulenta	5	S	W	LM,TEM,ITS,28S,*rbcL*
P. galaxiae	6	S	SU	LM,TEM,ITS, 28S, *rbcL*
P. mannii	14	I,S	SU,A	TEM,ITS, 28S,*rbcL*
P. multistriata	13	S	W	LM,TEM,ITS,28S,*rbcL*
P. pungens	6	S	SP,W	LM,TEM,ITS,28S,*rbcL*
P. subfraudulenta	3	I,S	A	LM,TEM,ITS

isolation data for station 0DB2 (Fig. 5).

P. calliantha Lundholm, Moestrup & Hasle (Fig. 6A-C)

The cells are linear in valve view (Fig. 6A) with the apical axis ranging between 68 and 82 µm and the transapical axis between 1.4 and 2.36 µm. A central larger interspace is present (Fig. 6B). The density of striae and fibulae in 10 µm ranges between 35 and 39 and between 18 and 22, respectively. Each stria contains one row of poroids, with 4–6 poroids in 1 µm (Fig. 6C). Poroids are segmented with 2–12 segments in each poroid, organised in a typical flower-like pattern (Fig. 6C).

P. mannii Amato & Montresor (Fig. 6D-F)

The cells resemble those of *P. calliantha*, but are typically longer and wider (Fig. 6D, Table 4). The two species are very hard to tell apart. The structure of the poroids is the only distinct characteristic; in *P. mannii*, they do not display flower-like organisation and are generally less segmented (2–7 sectors per poroid) (Fig. 6E, F).

P. delicatissima (Cleve) Heiden (Fig. 6G-I)

The cells are lanceolate in valve view (Fig. 6G) with the apical axis ranging between 20 and 76 µm and the transapical axis between 1.4 and 2.0 µm. A central larger interspace is present (Fig. 6I). The density of striae and fibulae in 10 µm ranges between 35 and 40 and between 18 and 26, respectively. Each stria contains two rows of poroids with 8–12 poroids in 1 µm (Fig. 6I). Poroids are not segmented.

P. galaxiae Lundholm & Moestrup (Fig. 7)

Three distinct morphotypes of this species have been identified. In natural samples, the cells were mostly solitary, but the medium morphotype occasionally formed two-cell chains. The transapical axis of the three morphotypes were similar at the widest part and ranged between 1.3 and 2.8 µm, while the apical axis greatly differed, ranging between 45 and 57 µm, 24 and 40 µm and 8.5 and 11 µm for the largest (Fig. 7 A–E), medium (Fig. 7 J–M) and small (Fig. 7 F–I) morphotypes, respectively. The large morphotype was exclusively tapered towards the rostrate ends, while the medium and small morphotype showed greater variability in this characteristic. We also observed variability in the arrangement of poroids with some cells having them closely arranged along the interstriae (Fig. 7 H), while others having them densely scattered around the striae (Fig. 7E).

P. pungens (Grunow ex Cleve) Hasle (Fig. 8A-C)

The cells are linear-lanceolate (Fig. 8A, B). The apical axis ranges between 24 and 121 µm and the transapical axis between 2.4 and 4.2 µm. The central larger interspace is not present. The density of striae and fibulae in 10 µm ranges between 8 and 13 and between 8 and 14, respectively. Each stria contains two rows of unsegmented poroids (2–4/ µm) (Fig. 8C).

P. fraudulenta (Cleve) Hasle (Fig. 8D-F)

The cells are lanceolate (Fig. 8D). The apical axis ranges between 72 and 110 µm and the transapical axis between 4.0 and 6.5 µm. The central larger interspace is present (Fig. 8E). The density of striae and fibulae in 10 µm ranges between 21 and 24 and between 20 and 24, respectively. Each stria contains two rows of poroids (5–6/ µm), which have several segments (Fig. 8F).

P. subfraudulenta Hasle (Fig. 8G-I)

The cells are linear-lanceolate (Fig. 8G). The apical axis ranges between 65 and 106 µm and the transapical axis between 4.3 and 6 µm. The central larger interspace is present (Fig. 8H). The density of striae and fibulae in 10 µm ranges between 23 and 28 and between 12 and 17, respectively. Each stria contains two rows of poroids (5–6/ µm), which have several segments (Fig. 8I).

P. multistriata H.Takano (Fig. 8J-L)

The cells are lanceolate in valve view and sigmoid in girdle view with typically curved apical ends (Fig. 8J). The apical axis ranges between 34 and 60 µm and the transapical axis between 2.2 and 4.0 µm. The central larger interspace is not present. The density of striae and fibulae in 10 µm ranges between 36 and 46 and between 22 and 28, respectively. Each stria contains two rows of unsegmented poroids (5–7/ µm) (Fig. 8K, L).

Table 4
Morphometric measurements of strains isolated in the Gulf of Trieste.

Species	Apical axis (µm)	Transapical axis (µm)	CIS	Fibulae in 10µm	Rows of poroids per stria	Poroids in 1µm	Poroids in 1µm	Poroid sectors
P. calliantha	**68-88.2** *77.88 ± 3.67 (91, 6)*	**1.4-2.4** *2.47 ± 0.9 (86, 6)*	+	**16-22** *19.4 ± 1.4 (48, 6)*	**33-39** *36.9 ± 1.5 (48, 6)*	**1**	**4-6** *4.8 ± 0.5 (53, 6)*	**2–12** *7.4 ± 2.3 (62, 4)*
P. delicatissima	**60-63** *61.36 ± 0.81 (17, 3)*	**1.4-1.9** *1.64 ± 0.17 (11, 1)*	+	**22-26** *23.8 ± 1.7 (10, 1)*	**40-42** *40.9 ± 1 (10, 1)*	**2**	**10-12** *11 ± 0.9 (10, 1)*	
P. fraudulenta	**72-108** *92.4 ± 9.23 (20, 2)*	**4.1–8.3** *5.87 ± 0.86 (20, 2)*	+	**20-24** *21.6 ± 1.2 (18, 2)*	**21-25** *23.1 ± 1 (18, 2)*	**1-2**	**5-7** *5.8 ± 0.6 (20, 2)*	**4-8** *6.1 ± 1.2 (18, 2)*
P. galaxiae	**8.5-57.4** *30.96 ± 14.12 (42, 6)*	**1.3-2.8** *2.01 ± 0..32 (43, 6)*	+	**20-30** *23.8 ± 3.1 (38, 6)*	**50-70** *59.6 ± 3.9 (38, 6)*	many	n.d.	n.d.
P. mannii	**57-107.7** *89.93 ± 6.33 (242, 10)*	**1.5-2.9** *1.98 ± 0.31 (157, 11)*	+	**14-25** *19.6 ± 2 (83, 11)*	**32-39** *35.3 ± 1.6 (93, 11)*	**1**	**4-6** *4.6 ± 0.6 (105, 11)*	**2-7** *4.2 ± 1.5 (51, 3)*
P. multistriata	**30-60** *50.15 ± 7.48 (45, 4)*	**2.4-4.6** *3.35 ± 0.51 (45, 4)*	–	**24-28** *25.3 ± 1.2 (29, 4)*	**34-45** *38.7 ± 2.3 (29, 4)*	**2**	**7-13** *10.7 ± 1.17 (29, 4)*	not segmented
P. pungens	**80-92** *86.21 ± 3.66 (24, 3)*	**2.7-5.9** *3.75 ± 0.96 (24, 3)*	–	**9-13** *11.4 ± 1.2 (10, 1)*	**10-13** *11.2 ± 0.9 (10, 1)*	**2**	**2-4** *2.97 ± 0.45 (35, 1)*	not segmented
P. subfraudulenta	**88.6-134** *112.16 ± 15.8 (72, 3)*	**3.5-6.5** *4.57 ± 0.86 (40, 3)*	+	**13-18** *14.9 ± 1.2 (18, 3)*	**24-25** *24.2 ± 0.4 (22, 3)*	**2**	**4-6** *5.1 ± 0.46 (33, 3)*	**3-7** *5.2 ± 1.3 (17, 1)*

CIS: central interspace. Range of values in bold; means ± SD in italics; number of measurements and number of strains measured in parentheses; n.d.: no data.

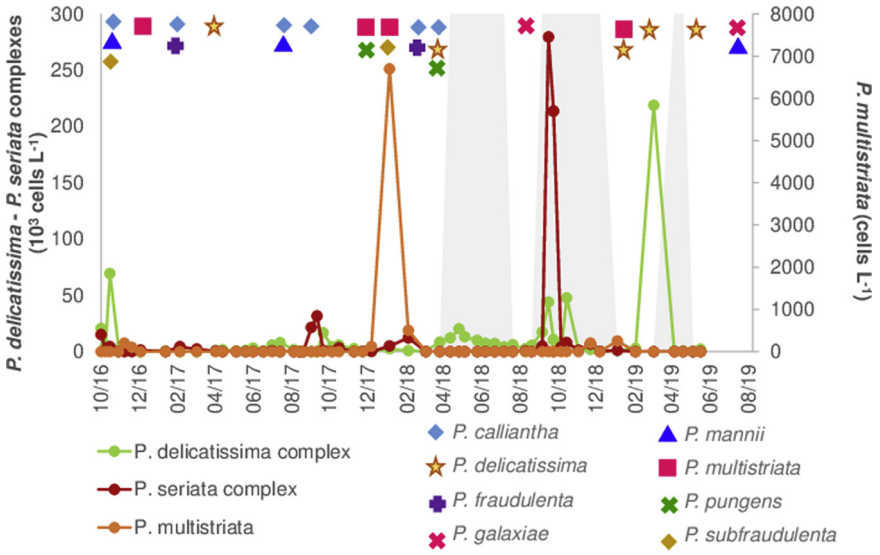

Fig. 5. Temporal distribution of abundances of *Pseudo-nitzschia* taxa identified in LM (lines) at 0DB2 station in the Gulf of Trieste from October 2016 to August 2019 and presence of species isolated and identified by molecular analysis (symbols). Grey-shaded areas indicate periods where isolations were not conducted.

3.3. Phylogenetic inference based on ITS2, 28S and rbcL

Because the ITS segment is very variable and only ITS2 sequences were available from the Italian strains, we constructed the phylogenies based on the ITS2 marker only, while the entire ITS region was sequenced and the sequences deposited in GenBank. The reconstructed phylogenies grouped our strains into 8 species (Figs. 9–11). We were unable to obtain *rbcL* sequences of *P. subfraudulenta*. The overall average *p*-distances were as follows: 28S: 0.033, *rbcL:* 0.053, ITS2: 0.179. Clearly, ITS2 was the most divergent marker despite having the shortest alignment of all markers used. There were some discrepancies among the different markers, particularly for the *calliantha/mannii* clade. The resolution of the two species concerned is supported by all three markers, but for the *rbcL* phylogeny neither *P. mannii* nor *P. calliantha* clades are sufficiently supported, although the group as a whole is monophyletic with high support. The *rbcL* phylogeny (Fig. 9) constructed in this study comprised of 22 species (40 % of described) of *Pseudo-nitzschia* and included *Fragilariopsis kerguelensis* that, unlike in the 28S phylogeny and the ITS2 phylogeny, clusters outside the *Pseudo-nitzschia* genus. We note that the groups defined by Lim et al. (2018) are well-recovered with monophyletic Groups I, II and III, even though Group II is only represented by *P. caciantha. P. fryxelliana*, sister taxa to the *P. fraudulenta* group clusters next to Group IV, which in this case is polyphyletic. The *rbcL* marker was also able to detect intraspecific variation, with the resolution comparable to ITS2 (Fig. 11) and better compared to the 28S marker (Fig. 10).

Intraspecific variation is apparent in the ITS2 and *rbcL* trees for *P. pungens, P. delicatissima, P. multistriata* and *P. galaxiae.* With 28S, intraspecific variation is detected only in *P. delicatissima* and to a limited extent in *P. galaxiae*, but interestingly not in *P. pungens*, which includes three described varieties. In addition, there is some variation in *P. calliantha*, which has also been revealed in the ITS2 phylogeny. As far as our strains are concerned, there is no pronounced variation between strains of the same species. The only exception is *P. galaxiae*; two strains isolated from the same net tow belong to two different clades in the *rbcL* phylogeny (Fig. 9) as well as in the ITS phylogeny (Fig. 11). On the contrary, although the 28S marker recognizes several clusters (ribotypes) within the *P. galaxiae* group with varying degrees of support (Fig. 10), our two strains fall within the same cluster. The mean *p*-distance (0.021) in the ITS2 marker between *P. galaxiae* strains, including those isolated in this study, is larger than the distances between some species (e.g. the mean distance between *P. sabit* and *P. decipiens* is 0.019). The same is true for the *rbcL* marker where the mean *p*-distance between *P. galaxiae* strains is 0.015, while *P. calliantha* and *P. mannii* are only separated by a mean *p*-distance of 0.006. Strains of *P. galaxiae* and *P. delicatissima* isolated in 2019 were not included in the phylogenetic trees, while only the *rbcL* of the former and both the ITS and *rbcL* of the latter were obtained.

Lastly we would like to point out the phylogenetic tree reconstructed with the 312bp-long *rbcL* barcode region (S3), which shows almost identical recovery of both species and strains compared to the 1220bp-long alignment. The support levels were somewhat lower and the delineation of *P. linea* and *P. americana*, which are very closely related, was not achieved. Otherwise, the barcode performs very well, and even recovers the strain diversity within *P. galaxiae*.

3.4. Network analysis and the distribution of Mediterranean Pseudo-nitzschia species

The grouping and connections of sequences based on statistical parsimony, coupled with geographical data in TCS networks, are presented in Fig. 12. More sequences were used in this analysis compared to the phylogenetic analysis (392, 258bp for ITS2, and 111, 1219 for *rbcL*), including the recently described *P. qiana* and *P. chiniana* (ITS2), and the additionally sequenced strains of *P. galaxiae* (*rbcL* only) that we isolated in August and September 2019. There were 68 and 78 parsimony-informative sites in the *rbcL* and ITS2 networks, respectively. The nucleotide diversity in the ITS2 network was much higher than in the *rbcL*. In both networks, the Mediterranean species with haplo and ribotype clusters, without representative Mediterranean strains, are only *P. pungens* (*P. pungens* 2, Fig. 12A; *P. pungens* 2–3, Fig. 12B) and *P. delicatissima* (*P. delicatissima* 2–3, Fig. 12A; *P. delicatissima* 2, Fig. 12B) with the addition of a single *P. multistriata* haplotype of non-Mediterranean origin present in the *rbcL* network. Of course, many species are yet to be found in the Mediterranean Sea, as evidenced by both networks, although some species have already been identified but lack the representative sequence data. Ten species with representative *rbcL* sequences were obtained from Mediterranean strains alone. The *rbcL* dataset is well-represented by Mediterranean strains, with nearly all the species identified in the basin being sequenced for this marker. The only exception is *P. subfraudulenta.* We were also unable to obtain quality *rbcL* sequences for this species. The networks are generally congruent with the Bayesian phylogenies, with considerable substructure seen particularly in Group IV, especially in *P. galaxiae* and *P. delicatissima* in

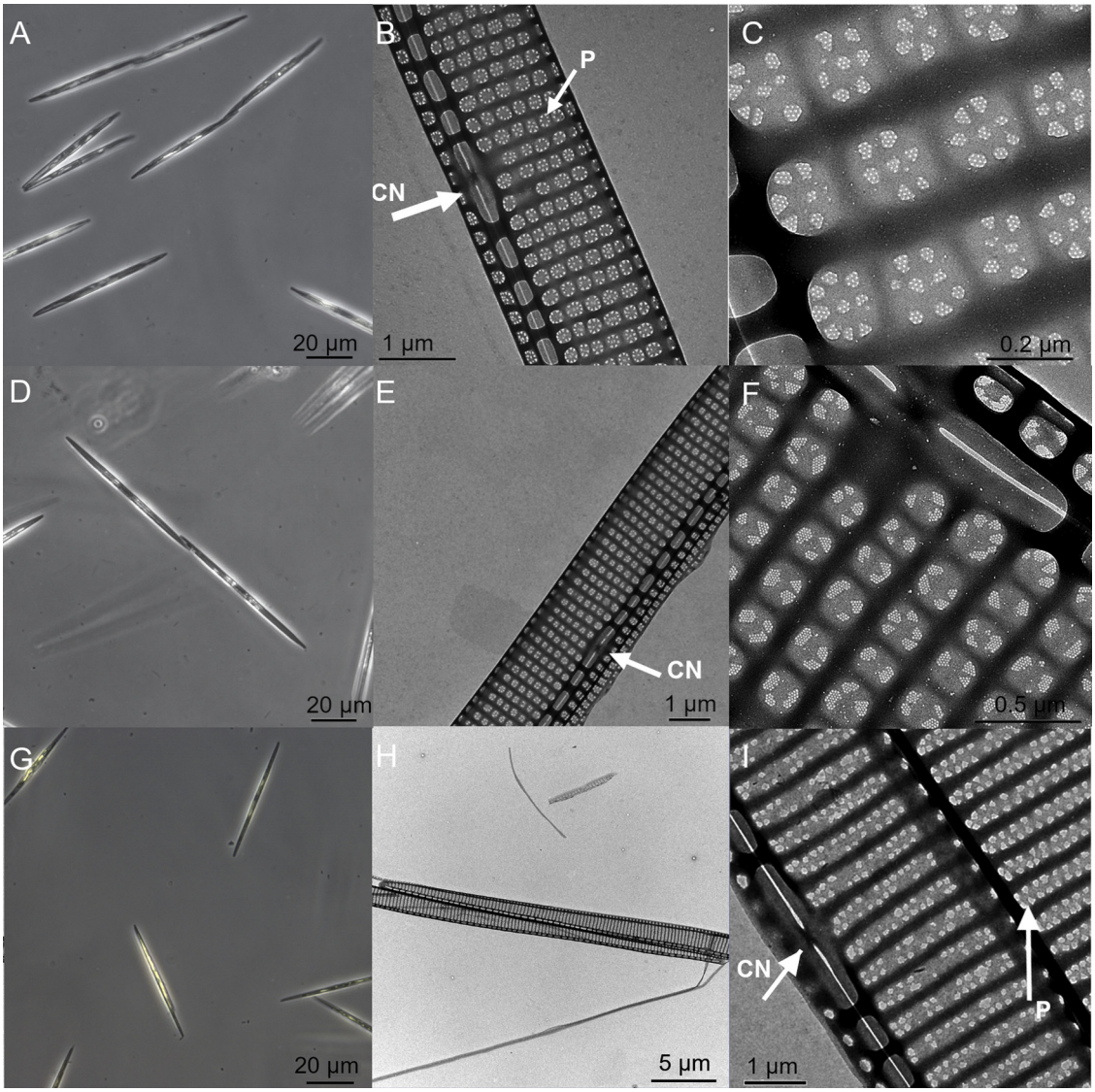

Fig. 6. Micrographs of *Pseudo-nitzschia* species identified in the Gulf of Trieste: *P. calliantha* (A–C), *P. mannii* (D–F), *P. delicatissima* (G–I). (A) Live cells, single and in chains, LM. (B) Central part of the valve showing the presence of the central nodule (CN) and poroid (P) organization (arrows), TEM. (C) Detail of poroid structure, TEM. (D) Girdle view of live cells in chain, LM. (E) Central part of the valve showing the presence of the central nodule (CN, arrow), TEM. (F) Detail of poroids showing the radial arrangement of sectors, TEM. (G) Single live cells, LM. (H) Part of the valve, TEM. (I) Central part of the valve showing the presence of the central nodule (CN) and two rows of poroids (P) (arrows), TEM.

both networks (Fig. 12A, B), as well as the *decipiens/sabit* group in the ITS2 network. Mediterranean strains, including the ones obtained in this study, generally cluster together and constitute a part of the main global haplotypes, with some notable exceptions. The first is the *P. delicatissima* group 1, which contains only Mediterranean strains. Likewise, strains of *P. brasiliana* from the NE and the NW Mediterranean form distinct haplogroups from the main haplogroup, but also between themselves (Fig. 12A). Other distinct Mediterranean haplotypes are seen in *P. calliantha* with two and *P. arenysensis* with several slightly different strains from the main haplogroup. There is also a haplogroup comprising strains of *P. dolorosa* and *P.* cf. *delicatissima* from the NE Mediterranean (*P. del.* 4, Fig. 12A), which is probably a cryptic species within the *P. delicatissima* complex. As noted in the previous section, the great diversity within *P. galaxiae* is also reflected at the geographical level, although we lack non-Mediterranean strains for comparison. There is a large haplogroup that comprises strains from GoT, NW and NE Mediterranean coastal waters in the ITS2 network (Fig. 12A), while in the *rbcL* all known haplotypes were recovered in GoN, NE Mediterranean strains group into one haplogroup, and our strains cluster into 4 haplogroups together with GoN strains (Fig.12B). Note the additionally sequenced strains isolated from Slovenia, that were not shown in the phylogeny.

4. Discussion

This study introduces an integrated approach combining molecular, ultrastructural and long-term monitoring data to describe the seasonal variation and diversity of *Pseudo-nitzschia* in a shallow gulf in the northern Adriatic Sea. We re-evaluated the power of several markers (28S, ITS2 and *rbcL*) for diatom barcoding and examined the phylogenetic relationships of Mediterranean and non-Mediterranean strains of *Pseudo-nitzschia* in order to fill knowledge gaps for the purpose of future research and surveys.

4.1. Pseudo-nitzschia spp. in the GoT and why species complexes don't tell us enough

Pseudo-nitzschia species are an important component of the

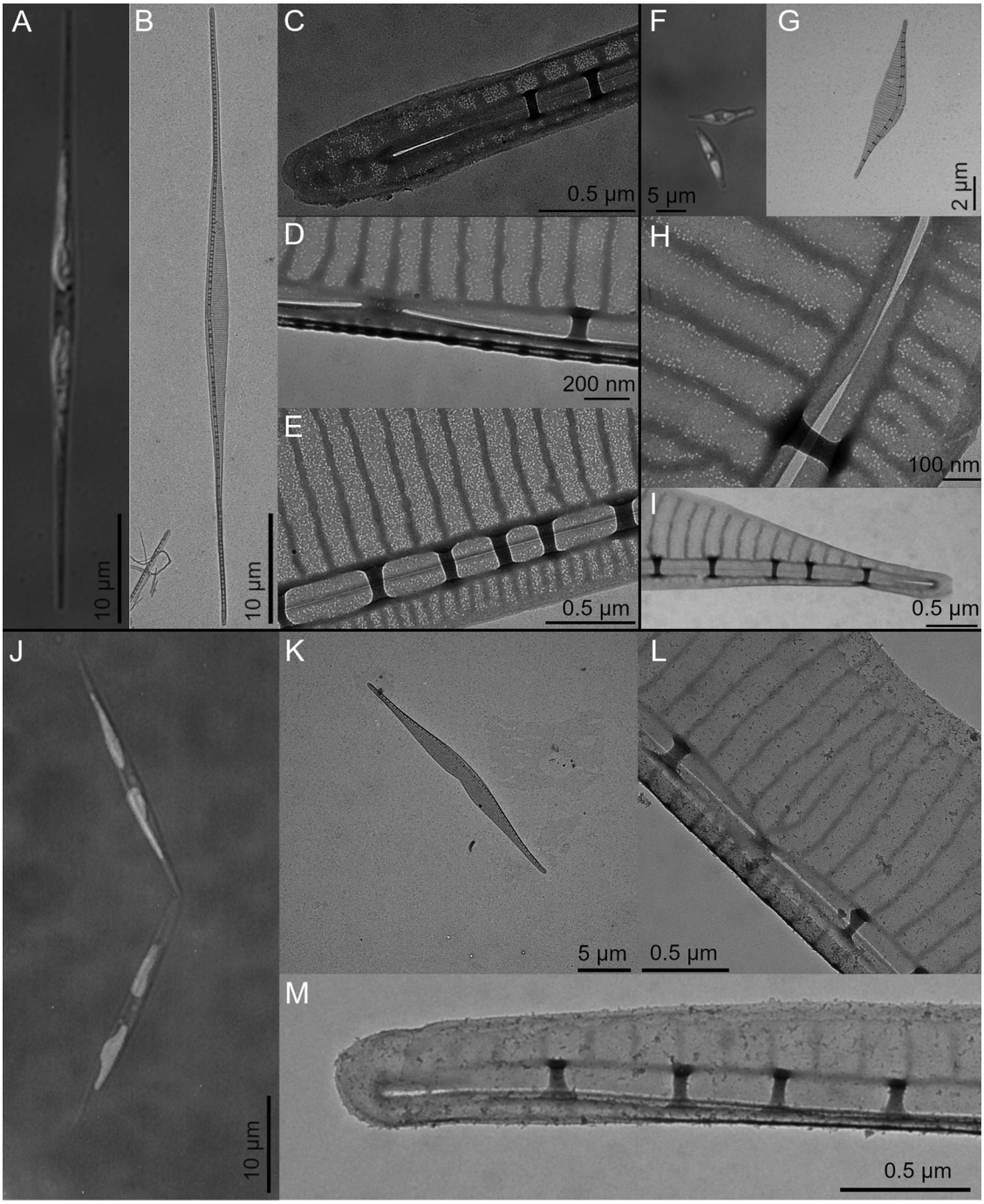

Fig. 7. Micrographs of *Pseudo-nitzschia galaxiae* identified in the Gulf of Trieste: large (A–E), small (F–I) and medium (J–M) morphotype. (A) Single live cell, LM, DIC-UV. (B) Valve of a long-sized specimen, TEM. (C) Apical end of a valve, TEM. (D) Central part of a valve with the central nodule, TEM. (E) Detail of a valve showing the typical and scattered poroids, TEM. (F) Live cells, LM, DIC-UV. (G) Valve of a small-sized specimen, TEM. (H) Central part of a valve showing the central nodule and poroids closely arranged along the interstriae, TEM. (I) Apical end of a valve, TEM. (J) Medium-sized specimens, LM, DIC-UV. (K) Valve of a medium-sized specimen, TEM. (L) Central part of a valve with the central nodule, TEM. (M) Apical end of a valve, TEM.

phytoplankton community all over the world (Viličić et al., 2009; Trainer et al., 2012; Bates et al., 2018; Mozetič et al., 2019). In a comparison of the phytoplankton community in port areas across the Adriatic Sea, *Pseudo-nitzschia* species as a whole were found to represent the core of the community in autumn and winter (Mozetič et al., 2019). Our time series analysis showed pronounced autumn blooms taking place annually and comprising up to 80 % of the total phytoplankton communities. Occasional spring blooms were also observed, but they usually represented smaller proportions of the phytoplankton community. Summer-autumn blooms of *Pseudo-nitzschia* are not surprising and have been documented in many regions including the Adriatic, Mediterranean, NE Atlantic and NE Pacific (Trainer et al., 2002; Mercado et al., 2005; Fehling et al., 2006; Ljubešić et al., 2011) and can represent significant portions of the phytoplankton communities (Quijano-Scheggia et al., 2008a). In our study, the number of cells occasionally reached over 10^6 cells L^{-1}, which is above management thresholds in areas where amnesic shellfish poisoning is a reoccurring problem (Trainer et al., 2002). These numbers are also higher than those reported from other areas in the Mediterranean (Mercado et al., 2005; Quijano-Scheggia et al., 2008a; Marić et al., 2011). However, in

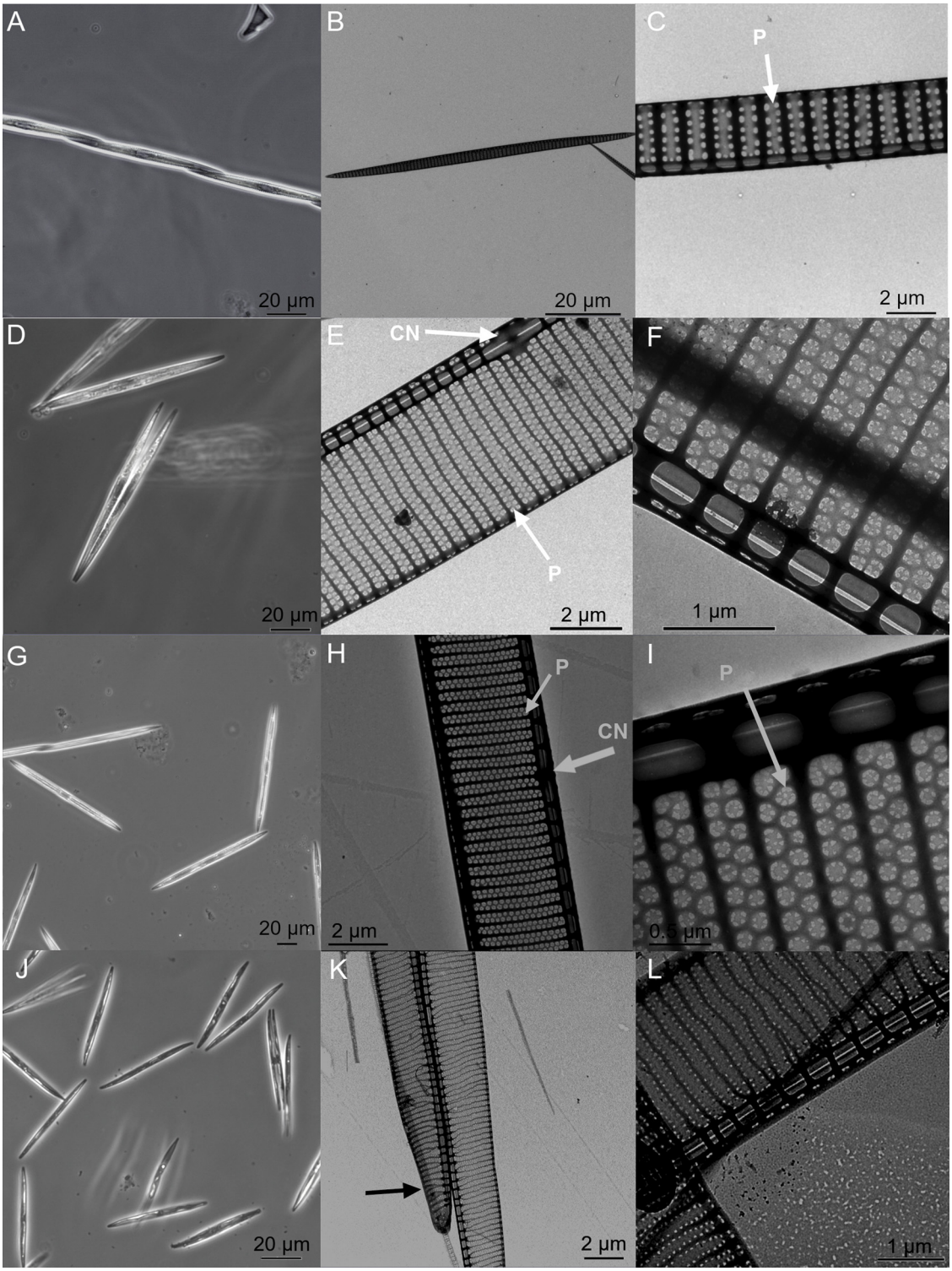

Fig. 8. Micrographs of *Pseudo-nitzschia* species identified in the Gulf of Trieste: *P. pungens* (A–C), *P. fraudulenta* (D–F), *P. subfraudulenta* (G–I) and *P. multistriata* (J–L). (A) Live cells in chains, LM. (B) Lanceolate cell, TEM. (C) Central part of the valve showing the poroid (P) organization (arrow), TEM. (D) Single live cells, LM. (E) Central part of the valve showing the presence of the central nodule (CN, arrow) and two rows of poroids (P, arrow), TEM. (F) Detail of poroids, TEM. (G) Single live cells, LM. (H) Central part of the valve showing the presence of the central nodule (CN) and two rows of poroids (P) (arrows), TEM. (I) Detail of poroids (P) (arrow), TEM. (J) Single live cells, LM. (K) The curved apical part of the valve (arrow), TEM. (L) Central part of the valve showing two rows of poroids, TEM.

terms of site management, the number of cells of a given complex is in itself not informative because toxin producers and non-producers can be simultaneously included in the count. The species complexes in the PCA demonstrate some seasonal preference, which is also in accordance with the isolation data, but the observed effects are stronger with the very reliable *P. multistriata* counts. *P. delicatissima* complex and *P.* cf. *galaxiae* seem to show the same seasonal preference. This may not be surprising since *P. galaxie* cells are also included in the complex counts. On the other hand problems of identification cannot be excluded, and *P.* cf. *galaxie* most likely constitutes more than one species of the *P.*

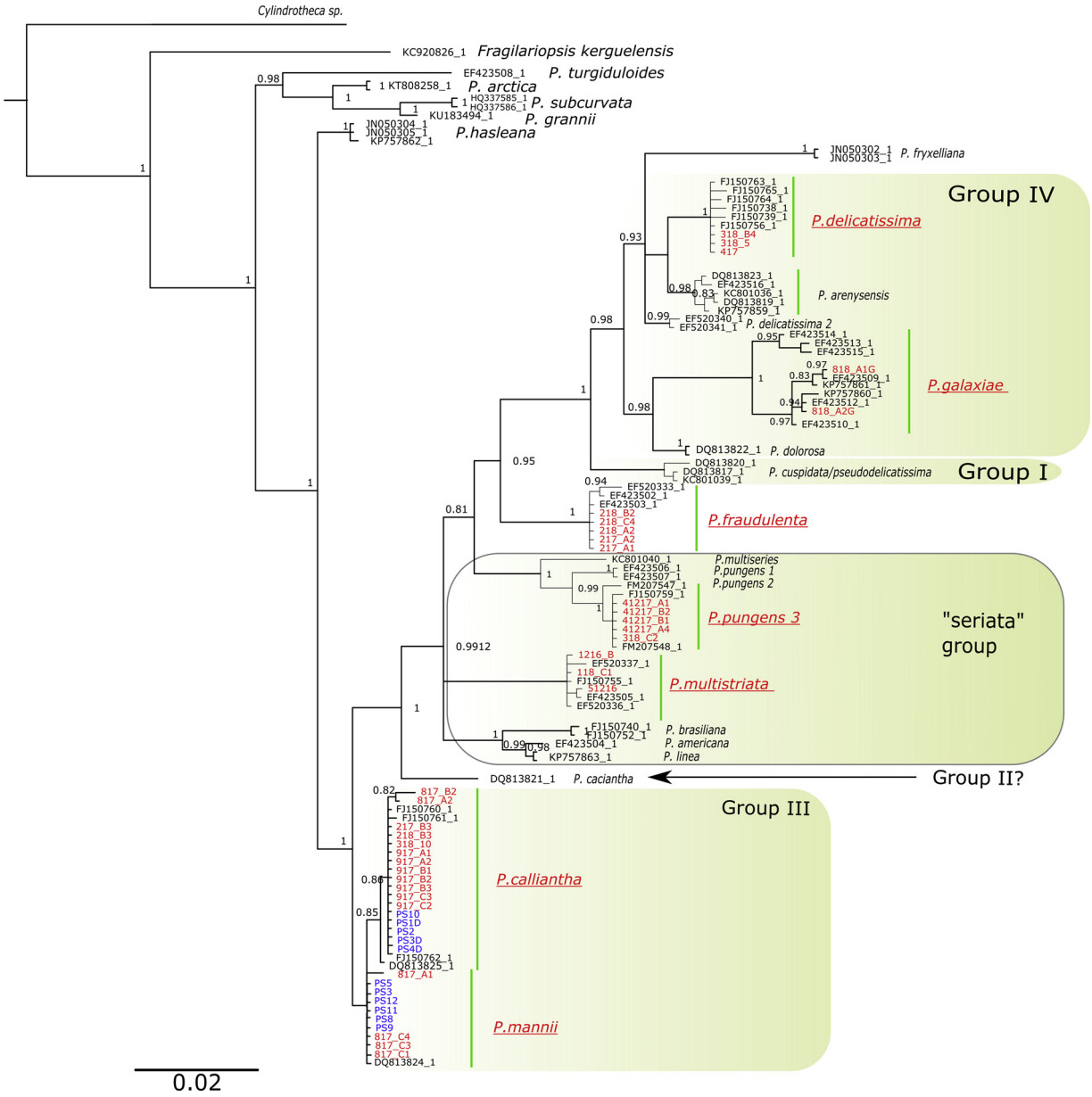

Fig. 9. Phylogenetic tree reconstruction using Bayesian inference on the *rbcL* marker GTR + I+G; ngen = 5,000,000. Identical sequences were removed from the tree and only representative strains retained. Species that have our native strains assigned to them are shown in enlarged and underlined red text. Bayesian posterior probabilities (PP) higher than 0.8 are shown on nodes. Strain names coloured in red represent isolates from Slovenia, while those coloured in blue represent isolates from Italy. Green shaded areas correspond to species groups defined by Lim et al. (2018). Group II is only represented by *P. caciantha.* Accession numbers of all of the used sequences are provided in supplementary material (Supplementary Table 2).

delicatissima complex, hence the similar ecological preference.

There is contrasting evidence of which environmental conditions promote the blooming of the different species complexes. Particular species may show different affinities to environmental parameters than their representative complexes, and this may be the actual source of the discrepancies between published literature. For example, Thorel et al. (2017) link the occurrence of *P. delicatissima* to low Si:N ratios whereas a negative correlation is observed for the *P. delicatissima* complex in regards to nitrate for the same study region (Downes-Tettmar et al., 2013). In our analysis, the *delicatissima* complex was correlated with high temperatures and lower phosphate concentrations, which could also signify nutrient uptake. Our PCA showed evident partitioning of the two species complexes that was mostly influenced by temperature and salinity; however, no marked seasonality was observed. These results are contradictory to the analysis of Fehling et al. (2006) that shows a preference of *P. seriata* complex for warmer waters (summer bloom), although the oceanographic conditions in the NE Atlantic are fundamentally different than those of our study area. However, the study area is most likely not the only factor explaining the different patterns of seasonal occurrence. We assume that a great deal of these discrepancies stem from the fact that several species with different ecological affinities are grouped together, and the groups, i.e. the complexes are then treated as single ecological units. Depending on the study area, different species are inherently assigned to the two complexes. Additionally, since cells are assigned to complexes based on valve widths, unnoticed cell division can double the width of the valve thus allowing for incorrect assignment of the complex. Our studied locations hosted at least four species of the *delicatissima* complex. The *seriata* complex is also represented by four species that all occur at similar times of the year, from early autumn to spring. Finally, we did not observe any

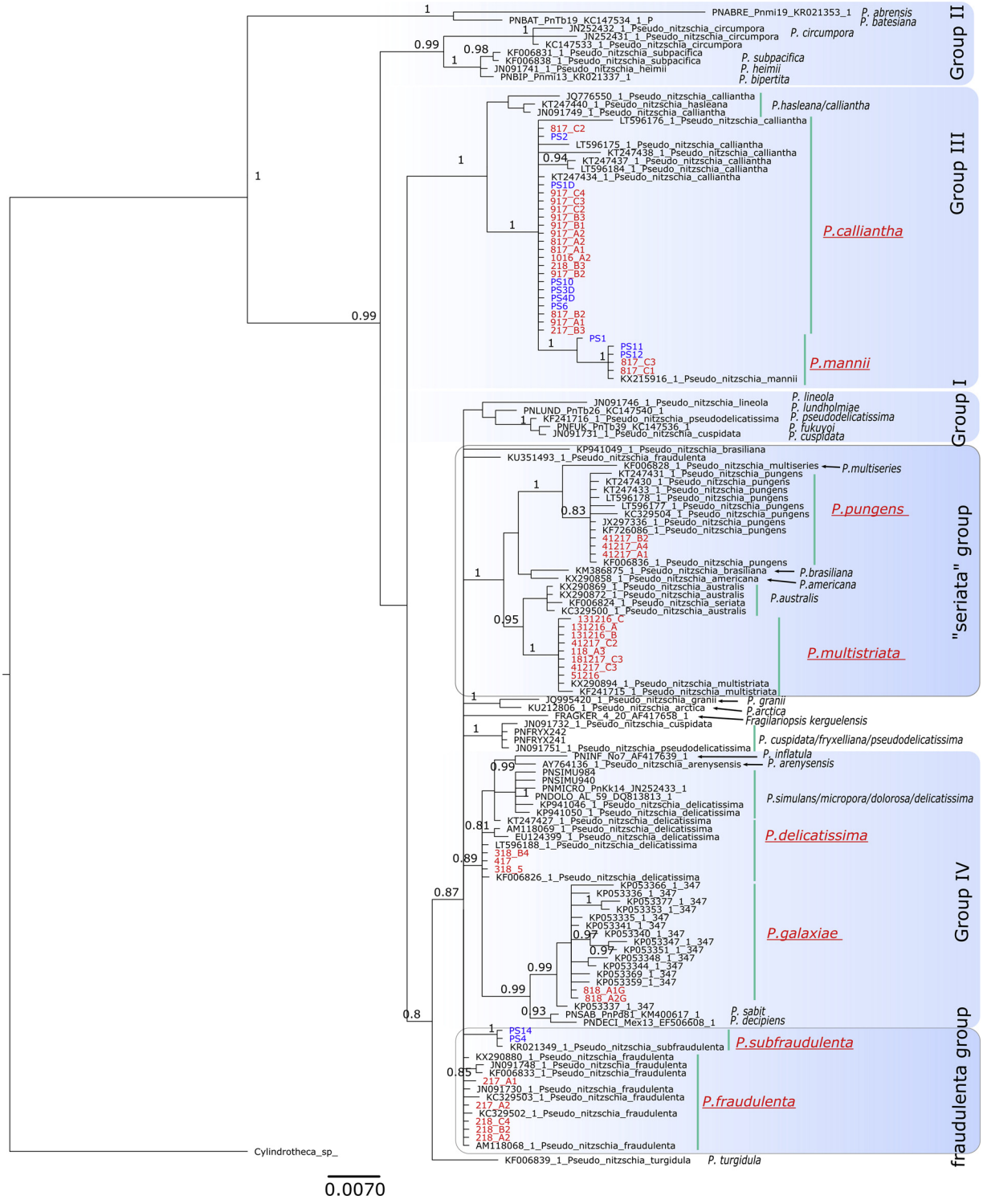

Fig. 10. Phylogenetic tree reconstruction using Bayesian inference on the 28S marker GTR + I+G, ngen = 10,000,000. Identical sequences were removed from the tree and only representative strains retained. Species that have our native strains assigned to them are shown in enlarged and underlined red text. Bayesian posterior probabilities (PP) higher than 0.8 are shown on nodes. Strain names coloured in red represent isolates from Slovenia, while those coloured in blue represent isolates from Italy. Blue shaded areas correspond to species groups defined by Lim et al. (2018). Accession numbers of all of the used sequences are provided in supplementary material (Supplementary Table 2).

pronounced seasonality from the NMDS either (S2), although the species complexes separated nicely, whereas the species constituting these complexes and for which data were available had fundamentally different ordinations in the multivariate space. This finding further stresses the importance of knowing the species when ecological explanations are to be drawn.

4.2. Unraveling the complex

To establish a benchmark for regional species diversity and seasonal occurrence, monthly isolations were performed. We concur that this is a stochastic approach that may not capture the entire community present at a given sampling point and is effort-biased. Nevertheless, in the

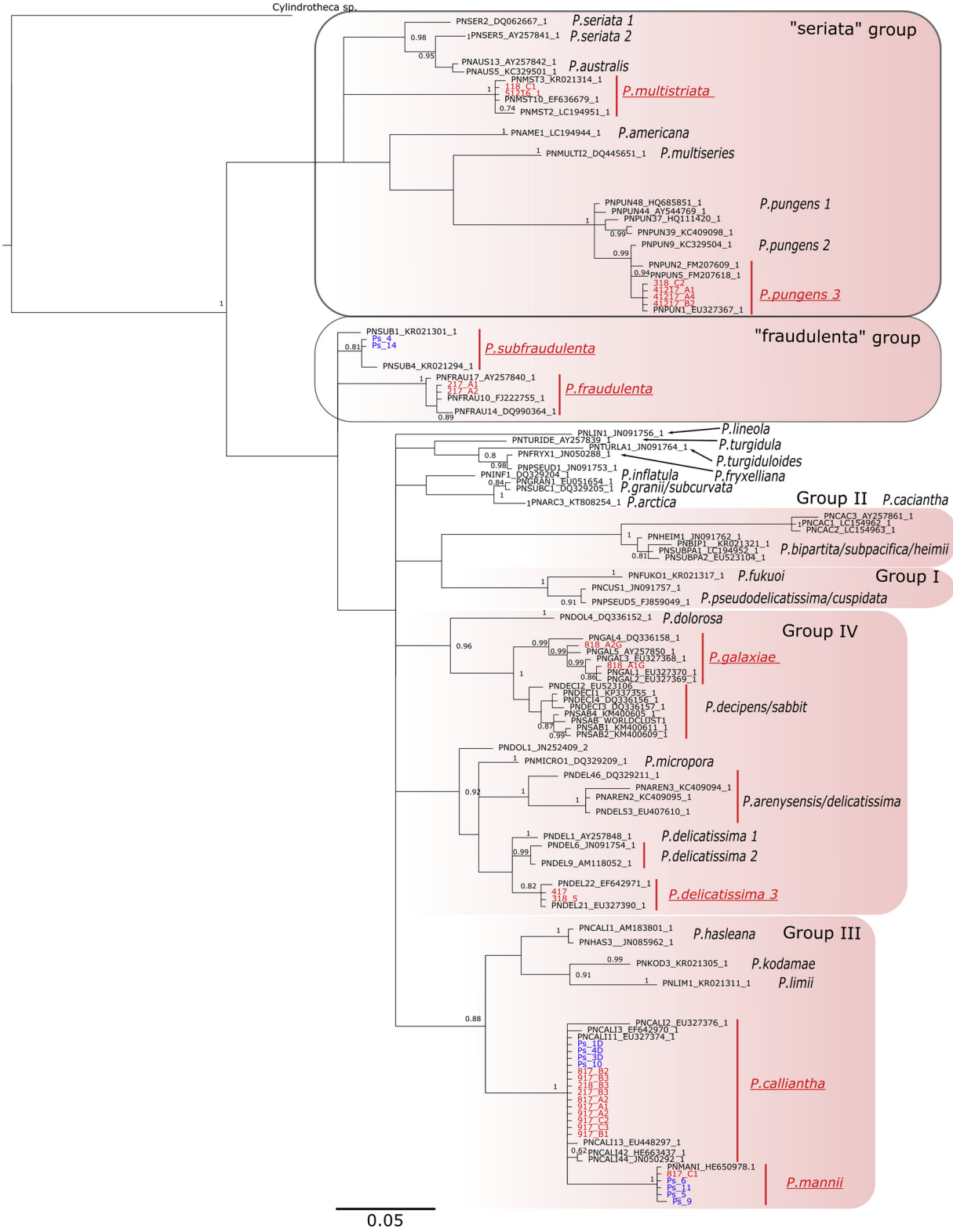

Fig. 11. Phylogenetic tree reconstruction using Bayesian inference on the ITS2 marker GTR + I+G; ngen = 10,000,000. Identical sequences were removed from the tree and only representative strains retained. Species that have our native strains assigned to them are shown in enlarged and underlined red text. Bayesian posterior probabilities (PP) higher than 0.8 are shown on nodes. Strain names coloured in red represent isolates from Slovenia, while those coloured in blue represent isolates from Italy. Red shaded areas correspond to species groups defined by Lim et al. (2018). Strain names coloured in red represent isolates from Slovenia, while those coloured in blue represent isolates from Italy.

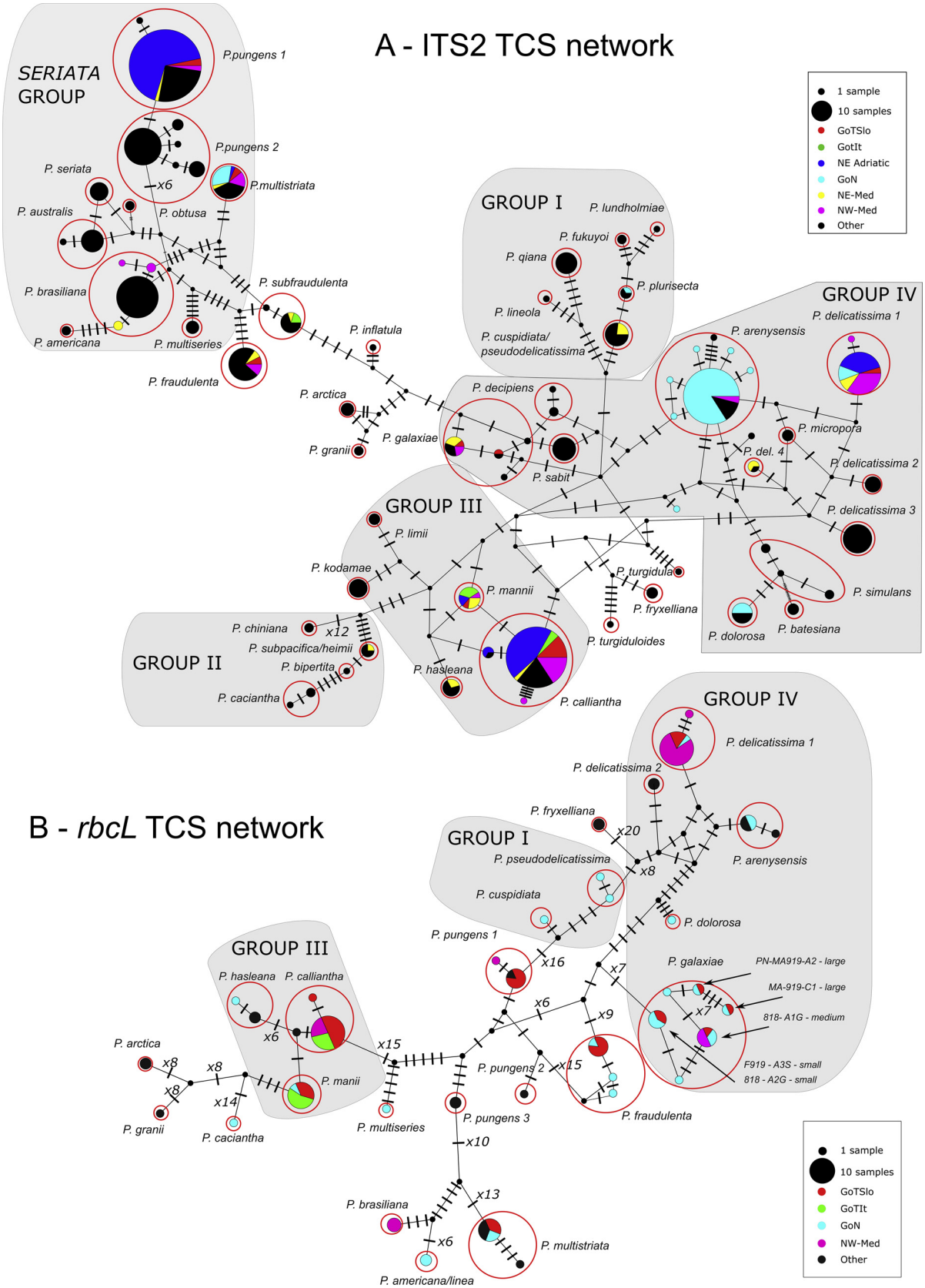

Fig. 12. TCS maximum parsimony networks constructed with (A) ITS2; 68 parsimony-informative sites; nucleotide diversity $\pi = 0.14$ and (B) *rbcL;* 75 parsimony-informative sites; nucleotide diversity $\pi = 0.04$. Tick marks on branches represent point mutations. Wherever the number of mutations between two nodes exceeds 5, the number of mutations is written instead. Red circles encompass all present ribo/haplotypes of a given species. Species are grouped according to Lim et al. (2018). The colors of nodes correspond to the geographic origin of the sequence, where all sequences that do not belong to the Mediterranean are colored in black.

survey starting in October 2016 and ending in March 2018 with some additional sampling in August 2018 and 2019 as well as January and February 2019, eight species were identified from 83 isolated strains combining morphological and molecular analyses: *P. calliantha*, *P. delicatissima*, *P. fraudulenta*, *P. galaxiae*, *P. mannii*, *P. multistriata*, *P. pungens* and *P. subfraudulenta*. These species had already been reported from the Adriatic Sea, in studies focusing on this genus (Lundholm et al., 2003; Caroppo et al., 2005; Burić et al., 2008; Marić et al., 2011; Penna et al., 2013; Arapov et al., 2016, 2017). *P. multistriata* and *P. galaxiae* are exceptions because they had been reported in long-term investigations based on LM (Cabrini et al., 2012; Cerino et al., 2012; Mozetič et al., 2019; Totti et al., 2019), but we lack TEM data for both while molecular data exist only for *P. multistriata* (Pistocchi et al., 2012). To our knowledge, this is the first unequivocal report of their presence, confirmed by ultrastructural and molecular evidence. In this study, we identify the Gulf of Trieste as a rich region for *Pseudo-nitzschia*, with eight species identified in a relatively short time. There are more than 16 species described in the GoN with a very long record of *Pseudo-nitzschia* studies (Ruggiero et al., 2015), eight species were recovered from the Bilbao estuary (Orive et al., 2013), 12 were found in a rather extensive area of the Greek coasts (Moschandreou et al., 2012), 10 along the Australian coasts (Ajani et al., 2013), more than 20 were described over the years in the NE Pacific and 22 were recovered by an integrated morphological-HTS approach in a recent study (Stern et al., 2018b).

Each species from a given sampling event has representative morphological image data. In this way we account for potential seasonal morphological variability if the species occurs in multiple seasons, as has been reported for *P. galaxiae* (Cerino et al., 2005). The obvious concern is that morphological variability may also exist within the same sampling event. Conversely to Cerino et al. (2005) we have demonstrated this for *P. galaxiae*. This variability may or may not be captured, depending on the success of isolation and subsequent identification. Morphologically, the isolated species resemble those in type descriptions or in other localities. The larger average size of *P. subfraudulenta* cells is noteworthy; on average, about 10 μm longer than those described in Malaysia (Teng et al., 2013) and almost 60 μm longer than those described in Greece (Moschandreou and Nikolaidis, 2010). Our measurements rely on three strains, two of which were smaller, on average, than the very long one. The morphometric signatures of other species are in line with published data. The only exceptions are the maximum widths of the valve in *P. mannii, P. calliantha, P. fraudulenta, P. pungens* and *P. multistriata.* However, these were outliers in the measurements and could be a consequence of unnoticed cell division, which in effect doubles the measured cell width.

Although the isolation date may not provide clear evidence on seasonal distribution, we have managed to obtain information from various resources, i.e. monitoring data, isolation date and TEM screens of natural samples taken during the monitoring program at the LTER station, in order to provide some insight regarding the seasonal dynamics of certain species. The occurrence of *P. multistriata*, which seems to be limited to December and January, is somewhat in accordance with Ribera d'Alcalà et al. (2004) who report a restricted 3–8 week occurrence of this species in the GoN, albeit in autumn. However, more recent work from this region notes a more widespread seasonal distribution of *P. multistriata* inferred from clone library reconstruction, including a late autumn-winter peak and a high summer peak (Ruggiero et al., 2015). We did not detect this species in summer in any of the samples. *P. delicatissima* was isolated and tentatively identified only in winter-early spring, which is similar to the GoN (Ribera d'Alcalà et al., 2004; Ruggiero et al., 2015), as well as with data from a recent study carried out in the Gulf of Seine (Thorel et al., 2017). The fact that the clonal library study by Ruggiero et al. (2015) detected multiple peaks spread across seasons is not surprising as the resolution of their method is much higher. Interestingly, their study also detected *P. fraudulenta* only in February, which is the only month in two consecutive years when viable cultures of this species were isolated during our study. *P. fraudulenta* was also found in early-spring cold water samples from other parts of the Mediterranean and the English Channel (Quijano-Scheggia et al., 2008b; Downes-Tettmar et al., 2013). Its sister taxon *P. subfraudulenta* was found in clonal libraries from the Tyrrhenian Sea only in autumn (Ruggiero et al., 2015), which is also in accordance with our isolation data linking this species to the period between October and December. This species is probably responsible for autumn blooms of the *seriata* complex, although this needs to be confirmed by other methods. *P. galaxiae* was isolated at the end of August and September and all three described morphotypes were present, while the morphotypes were found to be time-separated in the GoN (Cerino et al., 2005), even though most types were present in multiple seasons (Ruggiero et al., 2015). It should be noted, however, that small cells that could have belonged to *P. galaxiae* were observed in spring in our study as well, but isolation was not successful. Seasonal occurrence and inter-annual variability of phytoplankton species have been demonstrated to be heavily influenced by their biology. For example, microsatellite genotyping of *P. multistriata* in the GoN showed that two specific populations exist, living in sympatry and readily hybridizing, yet there is a bi-annual interchange of the dominant population (Tesson et al., 2014). This change is governed by their reproductive cycles that are influenced by cell size reductions and the existence of cell size optima for reproduction (D'Alelio et al., 2010). Thus, it may well be that the three distinct morphotypes of *P. galaxiae* that we found in the same spatio-temporal window are distinct populations at different stages of their life cycles that occur and bloom sympatrically in the ecological optimum for this species. These notions should be examined in light of the ability of the different *P. galaxiae* morpho-genotypes to reproduce, although increasingly smaller cells seem to lose this ability (D'Alelio et al., 2009). Genetically distinct sympatric or parapatric populations of planktonic protists have also been widely documented elsewhere, with varying degrees of hybridization, e.g. *Pseudo-nitzschia pungens* (Casteleyn et al., 2010), *Alexandrium fundysense, A. minutum* (Casabianca et al., 2011; Richlen et al., 2012), *Skeletonema marinoi* (Godhe and Härnström, 2010). The reason for genetic differentiation could be due to oceanographic feautures such as in *S. marinoi* or life-cycle characteristics such as resting stage formation or parasitism, as in *A. fundysense*. While there is no such apparent force in the Tyrrhenian Sea, Tesson et al. (2014) speculate that a meta-population model would explain the persisting existence of two or more interbreeding populations. Significant seasonal variability may have been missed by our study, since isolation data does not provide sufficient resolution of the community, unless effort is significantly increased (Bowers et al., 2018). Thus, to fully understand the seasonal profile of *Pseudo-nitzschia*, dedicated species-oriented techniques such as sandwich-hybridization, ARISA, qPCR or high-throughput sequencing, and where possible TEM/SEM screens of natural samples, should be used. For example, Bowers et al. (2018) have shown that by applying a species-oriented approach using a multitude of molecular and traditional techniques, a much better understanding of bloom dynamics is gained compared to the consideration of species complex data alone.

4.3. Phylogenies and the relationship of Adriatic strains with other Mediterranean isolates

While genetic characterization is crucial for correct identification of species and strains in the *Pseudo-nitzschia* genus, the selection of markers can sometimes lead to ambiguous results. The reason for this is the differential evolution rate among phylogenetic markers and perhaps even lineages, which emphasizes the importance of selecting multiple markers (Patwardhan et al., 2014). The majority of the strains that were sequenced in our study are associated with at least one genetic marker. Only *P. subfradulenta* from the Slovenian part of the GoT constitutes an exception. In the phylogenetic analysis, we focused on the recently published phylogenies of Lim et al. (2018) in order to compare our trees

and evaluate the power of the *rbcL* marker on a novel set of species, to our knowledge the most inclusive to date.

The groups defined in Lim et al. (2018) were all recovered in the ITS2 and 28S phylogenies although the tree structure is slightly different, which could be the consequence of strain selection, the fact that only Bayesian inference was used in this study, and the fact that the alignment of ITS2 was not guided by secondary structure. Groups were also recovered by *rbcL*, although Group II was only represented by *P. caciantha.* The *rbcL* marker compared to *cox1* used in Lim et al. (2018) has a better discriminative power, leading to a tree with greater support, although the overall *p*-distances are somewhat shorter. These were in agreement with Lim et al. (2018), with ITS2 showing the largest distances, followed by *rbcL* and 28S. The *rbcL* alignment was the longest of all three. Proper identification of species, using the molecular approach alone is somewhat problematic as can be seen in the relationship between *P. mannii* and *P. calliantha*. Phylogenetically, *P. manni* and *P. calliantha* are closely related and form a well-supported common clade according to all genetic markers. While in our analysis, one taxon was always parent to the other, the phylogenetic trees of Lim et al. (2018) place them as sister species. Moreover, according to the *rbcL*, the distance between the two taxa was smaller than the distance between strains of *P. galaxiae*, and also the separation between the two taxa was not supported by high posterior probability (PP). Nevertheless, *P. manni* has been successfully delineated from *P. calliantha* based on mating experiments and morphology (Amato and Montresor, 2008) However, it should be noted that prior to our study that recorded 15 different sequences, only one sequence of *P. mannii* was publicly available for *rbcL*.

In our case, the *rbcL* marker proved to be very versatile with high amplification success. The suitability of a 540-bp *rbcL* barcode has been evaluated in the past as regards the ability to distinguish *Pseudo-nitzschia* species (MacGillivary and Kaczmarska, 2011). The authors noted that the evaluated fragment is suitable especially in a dual-barcode system with ITS2, since they were unable to distinguish certain biologically distinct species (e.g. *P. calliantha* and *P. mannii*). Recently, a curated database for diatom *rbcL* barcodes was established based on a 312bp *rbcL* fragment (Rimet et al., 2016). Although the initial focus was on freshwater diatoms, many marine species are included and the use of the database in metabarcoding applications for monitoring the ecological status of water has been demonstrated (Vasselon et al., 2017). To illustrate the utility of this barcode, we produced a phylogenetic analysis based on this fragment. The recovery of the taxa was indeed almost identical to the 1220bp alignment (S3). This evaluation was done *in silico*; therefore, the entire amplification and sequencing process should be repeated using the selected barcode primers. The barcode should also be evaluated against a larger set of marine diatoms to fully understand its potential. So far, significantly less *Pseudo-nitzschia* species are sequenced for *rbcL* compared to ITS and 28S, but there are more compared to *cox1*. Of course, there is a relationship between the number of sequences and the variation detected but *rbcL* alignment had by far the least sequences and thus its discriminative power is apparent. 28S generally showed high amplification success in our study, but with much lower species resolution compared to ITS and *rbcL*. ITS is technically the most problematic, as it exists in multiple repeats in the genome, which could potentially be heterogenic (Orsini et al., 2004). This could impair PCR or result in unreadable sequences. Indeed, the amplification and sequencing success with this marker was the lowest, even though its discriminative power is the best.

While we detected some intraspecific variation among our strains this was limited. Only strains of *P. galaxiae*, which appears to be a species of great morphological as well as genetic variability (Cerino et al., 2005; D'Alelio and Ruggiero, 2015), are obviously different, as confirmed by this study. Interestingly, the two strains isolated from the same net sample and reported here, share a very similar 28S allele (Fig. 10), but have different ITS2 copies (Fig. 11) and cluster into different chloroplast haplogroups in the *rbcL* phylogeny (Fig. 9). Strain 818-A2 (small morphotype) even forms a unique branch in ITS2. The study by Cerino et al. (2005) examined the different morphotypes only with 28S and did not find significant differences between them, but it was noted that the morphotypes indeed differ in ITS (Ruggiero et al., 2015) while large differences in *rbcL* were also revealed although they were not backed by morphological data (D'Alelio and Ruggiero, 2015). Thus, it may well be that *P. galaxiae* is a species complex as was tentatively proposed before by Ruggiero et al. (2015). In the *rbcL* network, where recently isolated strains of *P. galaxiae* were also included, additional haplotypes were revealed, complementing those previously described elsewhere in the Mediterranean (*P. galaxie* cluster, Fig. 12B). The discrepancies between nuclear and plastid markers have been documented for other species of *Pseudo-nitzschia* as well. In *P. delicatissima*, Amato et al. (2007) demonstrated that the examined strains possessed two distinct *rbcL* haplotypes but had only one LSU and ITS genotype. These strains were able to interbreed successfully, and the authors postulated that different *rbcL* haplotypes can occur within single interbreeding populations. In *Pseudo-nitzschia*, inheritance of chloroplasts is bi-parental and recombination between chloroplasts was recorded for this genus including *P. galaxiae* (D'Alelio and Ruggiero, 2015). To further reveal the relationship of *P. galaxiae* strains in the Adriatic and in general, additional morphological and genetic studies should be conducted, including microsatellite genotyping, as well as a study of ITS2 secondary structure, which seems to be a good proxy for mating capability (Amato et al., 2007).

The genetic diversity among the Mediterranean strains is somewhat better captured with ITS2 compared to *rbcL*, which is not surprising given the number of sequences available (412 and 111, respectively). Furthermore, in the *rbcL* network, we observed that many species are only represented by Mediterranean strains; therefore, it is difficult to draw conclusions about genetic difference within and between the Mediterranean and other global regions. However, it should be reminded that the alignment used in the ITS2 network reconstruction was shorter since it was amended with gBlocks to aid alignment and remove gappy regions. Furthermore, strains may differ in one marker but be identical in another as was shown for *P. calliantha*, where strains differed in ITS1 but were identical in 5.8S-ITS2 (Lundholm et al., 2012). Some *Pseudo-nitzschia* species such as *P. pungens* are known cosmopolites, although it has been shown that distinct geographical partitioning backed by both morphological and genetic data exists for this species, where only one group out of three is in fact cosmopolitan (Casteleyn et al., 2010). This is also evident in our analysis with Mediterranean strains belonging to the globally distributed Clade I, and the geographically restricted clades II and III without Mediterranean members. A similar case is observed with *P. delicatissima* with two non-Mediterranean clades, although this species complex is less resolved and the two groups could well represent cryptic species. In contrast, *P. brasiliana* showed different haplogroups in ITS2 with a larger non-Mediterranean cluster and two Mediterranean ones. The differences between Catalan, Greek and other non-Mediterranean strains of *P. brasiliana* have already been discussed in Moschandreou et al. (2012). Finally, species represented by unique haplogroups that also include Mediterranean strains, including *P. multistriata, P. fraudulenta, P. mannii, P. hasleana, P. subpacifica, P. pseudodelicatissima/cuspidiata* and *P. pluriseca* could reflect a lack of sequencing effort on the one hand and the abscence of crypticism within these species on the other.

4.4. Integrating molecular and morphological data for better management of LTER sites

Traditional methods such as light microscopy are often insufficient to uncover cryptic protistian diversity, yet this is the most common method used for long-term monitoring for analyses of plankton community structure. While knowing the exact species or even ecotypes of a certain species may not be the goal of such monitoring, we should be more careful when potentially toxic species are concerned (Bickford

et al., 2007). The most notable example is perhaps the *Alexandrium tamarense* species complex, comprised of five species of which only some are producers of saxitoxin, and cannot be distinguished using light and even electron microscopy (John et al., 2014). Similarly, it was shown that distinct genetic varieties of *Akashiwo sanguinea* assume different ecological niches, but are morphologically undistinguishable (Luo et al., 2017). In *Pseudo-nitzschia*, HAB and LTER monitoring usually recovers only species complexes defined by valve width. Although morphological traits can be proxies for ecological preference as was shown in freshwater diatoms (Potapova and Hamilton, 2007), we are not aware of any research that shows valve width defines ecological preference in *Pseudo-nitzschia*. We thus question the serviceability of this data in terms of LTER site management and explore what can be gained from dedicated molecular surveys such as the one presented here. Incorporating molecular knowledge into LTER strategies allows for a better understanding of the local ecosystem and leads to better management (Stern et al., 2018b). Such efforts also help to build local reference databases of both sequence and biological data that can be then referred to in high-throughput sequencing studies, which are more reliable and robust (Stern et al., 2018a). Our data shows that the *P. delicatissima* complex, which we now know comprises of at least four species (*P delicatissima, P. calliantha, P. mannii* and *P. galaxiae*), preferentially occurs in summer and spring conditions, while the *seriata* complex (comprising of *P. multistriata, P. pungens, P. fraudulenta* and *P. subfraudulenta*) peaks in autumn. Until the current study was conducted, only species complex data and data on *P. multistriata* were available in the GoT. The three-year campaign of strain isolation followed by characterization and backtracking to LM data allowed us to understand the community much better and also enabled us to identify more species under LM because we now know which species can be expected at different times of the year. To demonstrate this, a proof-of-concept CCA analysis was conducted (S4 B) where we used the isolation data of each sampling event to quality check the count data (see S4 A for methodology). Backtracking was only done for the *seriata* complex because tentative counts of species that are grouped into this complex exist for LM, whereas the *delicatissima* complex is always reported as it is because the species are almost impossible to tell apart even with prior knowledge. *P. galaxiae* is an exception; its cells show some distinct features such as thin rostrae, while the small morphotype is also distinguishable. Nevertheless, the smaller morphotype often impedes detection due to its size and resembles many small planktonic and benthic diatoms, while the larger morphotype can from our experience be confused with *P. delicatissima*. The CCA showed the preference of *P. multistriata* and *P. pungens* for saltier, colder waters with higher concentrations of silicate and DIN, which represent typical winter conditions, while *P. fraudulenta* was associated with quite different conditions. Although, the number of samples in this analysis is small, we can see that the respective species complex of the aforementioned species ordinate differently than the species itself. Therefore, any discrepancies between species complex and species affinities to environmental conditions reported in Thorel et al. (2017) and previously discussed in this work, may not be surprising. We are convinced that decomplexing of the *P. delicatissima* complex would yield similar results, since we know that different species occur in different temporal windows. We believe our work feeds well into the framework of molecular data integration in routine monitoring proposed by Stern et al., 2018, and is thus an example of good practice, even though the resoluting power of our method was not the strongest. Many molecular tools can be used to gain better species resolution and seasonal profiles (e.g. qPCR: Andree et al., 2011; microarray: Smith et al., 2012; various SHA and FISH techniques: Orozco et al., 2016; Medlin and Orozco, 2017; Bowers et al., 2018), although the feasibility to use them in routine monitoring is often impaired due to budgetary and staff limitations. Yet, we must be careful when drawing conclusions on the affinities of different species to environmental conditions, since bloom phenology and species succession also depends on species interactions, nutrition and parasitism (Gleason et al., 2015; D'Alelio et al., 2019). Further studies and models of the seasonal distribution of individual species, including inter-annual difference, will help fill the knowledge gaps and help elucidate the ways in which species dominance and blooming relates to environmental and ecosystem conditions.

To conclude, we have demonstrated that by combining the molecular and morphological toolkit more reliable information on species diversity and seasonality can be established, which greatly improves monitoring strategies while enabling further ecological analyses.

Funding

The authors acknowledge the financial support from the Slovenian Research Agency (research core funding No. P1-0237 and program for young researchers, in accordance with the agreement on (co) financing research activities), the Friuli Venezia Giulia Region (L.R. 15/2005) and the Slovenian Environment Agency.

Declaration of Competing Interest

The authors declare that they have no known competing financial interests or personal relationships that could have appeared to influence the work reported in this paper.

Acknowledgments

The authors wish to thank Paolo Bertoncin (Department of Life Science, University of Trieste) for technical assistance with TEM. Station C1-LTER is part of the national and international Long Term Ecological Research network (LTER-Italy, LTER-Europe, ILTER). The authors would like to thank Bruno Cataletto, Cinzia Comici, Edvino Cociancich, Miljan Šiško and Tihomir Makovec for sampling and performing CTD measurements, Martina Kralj for nutrient data and Daniela Fornasaro and Miljan Šiško for phytoplankton data. The authors thank Valentina Torboli (Department of Life Science, University of Trieste) and the staff of the Laboratory for Evolutionary Ecology (Centre for Marine Research, Ruđer Bošković Institute) in Rovinj, Croatia for providing some ITS and 28S sequences of the Italian strains. Finally, we thank three anonymous reviewers who have helped to substantially improve this manuscript with their insight and suggestions.[CG]

Appendix A. Supplementary data

Supplementary material related to this article can be found, in the online version, at doi:https://doi.org/10.1016/j.hal.2020.101773.

References

Ajani, P., Murray, S., Hallegraeff, G., Lundholm, N., Gillings, M., Brett, S., Armand, L., 2013. The diatom genus Pseudo-nitzschia (Bacillariophyceae) in New South Wales, Australia: morphotaxonomy, molecular phylogeny, toxicity, and distribution. J. Phycol. 49, 765–785. https://doi.org/10.1111/jpy.12087.

Amato, A., Montresor, M., 2008. Morphology, phylogeny, and sexual cycle of Pseudo-nitzschia mannii sp. nov. (Bacillariophyceae): a pseudo-cryptic species within the P. pseudodelicatissima complex. Phycologia 47, 487–497. https://doi.org/10.2216/07-92.1.

Amato, A., Kooistra, W.H.C.F., Levialdi Ghiron, J.H., Mann, D.G., Pröschold, T., Montresor, M., 2007. Reproductive isolation among sympatric cryptic species in marine diatoms. Protist 158, 193–207. https://doi.org/10.1016/j.protis.2006.10.001.

Anderson, D., 2014. HABs in a changing world: a perspective on harmful algal blooms, their impacts, and research and management in a dynamic era of climactic and environmental change. In: Harmful Algae 2012 Proc. 15th Int. Conf. Harmful Algae Oct. 29 - Novemb. 2, 2012. CECO, Chang. Gyeongnam, Korea. Int. Conf. Harmful Algae (15th 2012 Chang. Gyeongnam, Kore. 2012. pp. 3–17.

Anderson, C.R., Sapiano, M.R.P., Prasad, M.B.K., Long, W., Tango, P.J., Brown, C.W., Murtugudde, R., 2010. Predicting potentially toxigenic Pseudo-nitzschia blooms in the Chesapeake Bay. J. Mar. Syst. 83, 127–140. https://doi.org/10.1016/j.jmarsys.2010.04.003.

Andree, K.B., Fernández-Tejedor, M., Elandaloussi, L.M., Quijano-Scheggia, S., Sampedro,

N., Garcés, E., Camp, J., Diogène, J., 2011. Quantitative PCR coupled with melt curve analysis for detection of selected Pseudo-nitzschia spp. (Bacillariophyceae) from the northwestern Mediterranean Sea. Appl. Environ. Microbiol. 77, 1651–1659. https://doi.org/10.1128/AEM.01978-10.

Arapov, J., Ujevic, I., Pfannkuchen, D.M., Godrijan, J., Bakrac, A., Gladan, Z.N., Marasovic, I., 2016. Domoic acid in phytoplankton net samples and shellfish from the krka river estuary in the central Adriatic Sea. Mediterr. Mar. Sci. 17, 340–350. https://doi.org/10.12681/mms.1471.

Arapov, J., Skejić, S., Bužančić, M., Bakrač, A., Vidjak, O., Bojanić, N., Ujević, I., Gladan, Ž.N., 2017. Taxonomical diversity of Pseudo-nitzschia from the Central Adriatic Sea. Phycol. Res. 65, 280–290. https://doi.org/10.1111/pre.12184.

Bates, S.S., Hubbard, K.A., Lundholm, N., Montresor, M., Leaw, C.P., 2018. Pseudo-nitzschia, Nitzschia, and domoic acid: new research since 2011. Harmful Algae 1–41. https://doi.org/10.1016/j.hal.2018.06.001.

Bickford, D., Lohman, D.J., Sodhi, N.S., Ng, P.K.L., Meier, R., Winker, K., Ingram, K.K., Das, I., 2007. Cryptic species as a window on diversity and conservation. Trends Ecol. Evol. (Amst.) 22, 148–155. https://doi.org/10.1016/j.tree.2006.11.004.

Bowers, H.A., Ryan, J.P., Hayashi, K., Woods, A.L., Marin, R., Smith, G.J., Hubbard, K.A., Doucette, G.J., Mikulski, C.M., Gellene, A.G., Zhang, Y., Kudela, R.M., Caron, D.A., Birch, J.M., Scholin, C.A., 2018. Diversity and toxicity of Pseudo-nitzschia species in Monterey Bay: perspectives from targeted and adaptive sampling. Harmful Algae 78, 129–141. https://doi.org/10.1016/j.hal.2018.08.006.

Burić, Z., Viličić, D., Mihalić, K.C., Carić, M., Kralj, K., Ljubešić, N., 2008. Pseudo-nitzschia blooms in the zrmanja river estuary (eastern adriatic sea). Diatom Res. 23, 51–63. https://doi.org/10.1080/0269249X.2008.9705736.

Cabrini, M., Fornasaro, D., Cossarini, G., Lipizer, M., Virgilio, D., 2012. Phytoplankton temporal changes in a coastal northern Adriatic site during the last 25 years. Estuar. Coast. Shelf Sci. 115, 113–124. https://doi.org/10.1016/j.ecss.2012.07.007.

Caroppo, C., Congestri, R., Bracchini, L., Albertano, P., 2005. On the presence of Pseudo-nitzschia calliantha Lundholm, Moestrup et hasle and Pseudo-nitzschia delicatissima (Cleve) Heiden in the Southern Adriatic Sea (Mediterranean Sea, Italy). J. Plankton Res. 27, 763–774. https://doi.org/10.1093/plankt/fbi050.

Casabianca, S., Penna, A., Pecchioli, E., Jordi, A., Basterretxea, G., Vernesi, C., 2011. Population genetic structure and connectivity of the harmful dinoflagellate Alexandrium minutum in the Mediterranean Sea. Proc. R. Soc. B Biol. Sci. 279, 129–138. https://doi.org/10.1098/rspb.2011.0708.

Casteleyn, G., Leliaert, F., Backeljau, T., Debeer, A.E., Kotaki, Y., Rhodes, L., Lundholm, N., Sabbe, K., Vyverman, W., 2010. Limits to gene flow in a cosmopolitan marine planktonic diatom. Proc. Natl. Acad. Sci. U. S. A. 107, 12952–12957. https://doi.org/10.1073/pnas.1001380107.

Castresana, J., 2000. Selection of conserved blocks from multiple alignments for their use in phylogenetic analysis. Mol. Biol. Evol. 17, 540–552. https://doi.org/10.1093/oxfordjournals.molbev.a026334.

Cerino, F., Orsini, L., Sarno, D., Dell'Aversano, C., Tartaglione, L., Zingone, A., 2005. The alternation of different morphotypes in the seasonal cycle of the toxic diatom Pseudo-nitzschia galaxiae. Harmful Algae 4, 33–48. https://doi.org/10.1016/j.hal.2003.10.005.

Cerino, F., Bernardi Aubry, F., Coppola, J., La Ferla, R., Maimone, G., Socal, G., Totti, C., 2012. Spatial and temporal variability of pico-, nano- and microphytoplankton in the offshore waters of the southern Adriatic Sea (Mediterranean Sea). Cont. Shelf Res. 44, 94–105. https://doi.org/10.1016/j.csr.2011.06.006.

Clement, M., Posada, D., Crandall, K.A., 2000. TCS: a computer program to estimate gene genealogies. Mol. Ecol. 9, 1657–1659. https://doi.org/10.1046/j.1365-294x.2000.01020.x.

Cozzi, S., Falconi, C., Comici, C., Čermelj, B., Kovac, N., Turk, V., Giani, M., 2012. Recent evolution of river discharges in the Gulf of Trieste and their potential response to climate changes and anthropogenic pressure. Estuar. Coast. Shelf Sci. 115, 14–24. https://doi.org/10.1016/j.ecss.2012.03.005.

D'Alelio, D., Ruggiero, M.V., 2015. Interspecific plastidial recombination in the diatom genus Pseudo-nitzschia. J. Phycol. 51, 1024–1028. https://doi.org/10.1111/jpy.12350.

D'Alelio, D., Amato, A., Kooistra, W.H.C.F., Procaccini, G., Casotti, R., Montresor, M., 2009. Internal Transcribed Spacer Polymorphism in Pseudo-nitzschia multistriata (Bacillariophyceae) in the Gulf of Naples: Recent Divergence or Intraspecific Hybridization? Protist 160, 9–20. https://doi.org/10.1016/J.PROTIS.2008.07.001.

D'Alelio, D., d'Alcalà, M.R., Dubroca, L., Sarn, D., Zingone, A., Montresor, M., 2010. The time for sex: a biennial life cycle in a marine planktonic diatom. Limnol. Oceanogr. 55, 106–114. https://doi.org/10.4319/lo.2010.55.1.0106.

D'Alelio, D., Hay Mele, B., Libralato, S., Ribera d'Alcalà, M., Jordán, F., 2019. Rewiring and indirect effects underpin modularity reshuffling in a marine food web under environmental shifts. Ecol. Evol. https://doi.org/10.1002/ece3.5641. ece3.5641.

Downes-Tettmar, N., Rowland, S., Widdicombe, C., Woodward, M., Llewellyn, C., 2013. Seasonal variation in Pseudo-nitzschia spp. And domoic acid in the Western English Channel. Cont. Shelf Res. 53, 40–49. https://doi.org/10.1016/j.csr.2012.10.011.

Fehling, J., Davidson, K., Bolch, C., Tett, P., 2006. Seasonally of Pseudo-nitzschia spp. (Bacillariophyceae) in western Scottish waters. Mar. Ecol. Prog. Ser. 323, 91–105. https://doi.org/10.3354/meps323091.

Fonda Umani, S., Del Negro, P., Larato, C., De Vittor, C., Cabrini, M., Celio, M., Falconi, C., Tamberlich, F., Azam, F., 2007. Major inter-annual variations in microbial dynamics in the Gulf of Trieste (northern Adriatic Sea) and their ecosystem implications. Aquat. Microb. Ecol. 46, 163–175. https://doi.org/10.3354/ame046163.

Gleason, F.H., Jephcott, T.G., Küpper, F.C., Gerphagnon, M., Sime-Ngando, T., Karpov, S.A., Guillou, L., van Ogtrop, F.F., 2015. Potential roles for recently discovered chytrid parasites in the dynamics of harmful algal blooms. Fungal Biol. Rev. 29, 20–33. https://doi.org/10.1016/j.fbr.2015.03.002.

Godhe, A., Härnström, K., 2010. Linking the planktonic and benthic habitat: genetic structure of the marine diatom Skeletonema marinoi. Mol. Ecol. 19, 4478–4490. https://doi.org/10.1111/j.1365-294X.2010.04841.x.

Hansen, H.P., Koroleff, F., 1999. Determination of nutrients, in: Methods of Seawater Analysis: Third, Completely Revised and Extended Edition. Wiley-VCH Verlag GmbH, Weinheim, Germany, pp. 159–228. https://doi.org/10.1002/9783527613984.ch10.

Huang, C.X., Dong, H.C., Lundholm, N., Teng, S.T., Zheng, G.C., Tan, Z.J., Lim, P.T., Li, Y., 2019. Species composition and toxicity of the genus Pseudo-nitzschia in Taiwan Strait, including P. chiniana sp. nov. and P. qiana sp. nov. Harmful Algae 84, 195–209. https://doi.org/10.1016/j.hal.2019.04.003.

John, U., Litaker, R.W., Montresor, M., Murray, S., Brosnahan, M.L., Anderson, D.M., 2014. Formal revision of the Alexandrium tamarense species complex (Dinophyceae) taxonomy: the introduction of five species with emphasis on molecular-based (rDNA) classification. Protist 165, 779–804. https://doi.org/10.1016/j.protis.2014.10.001.

Katoh, K., Standley, D.M., 2013. MAFFT multiple sequence alignment software version 7: improvements in performance and usability. Mol. Biol. Evol. 30, 772–780. https://doi.org/10.1093/molbev/mst010.

Kumar, S., Stecher, G., Tamura, K., 2016. MEGA7: molecular evolutionary genetics analysis version 7.0 for bigger datasets. Mol. Biol. Evol. 33, 1870–1874. https://doi.org/10.1093/molbev/msw054.

Lane, J.Q., Raimondi, P.T., Kudela, R.M., 2009. Development of a logistic regression model for the prediction of toxigenic pseudo-nitzschia blooms in monterey bay. California. Mar. Ecol. Prog. Ser. 383, 37–51. https://doi.org/10.3354/meps07999.

Leigh, J.W., Bryant, D., 2015. POPART: full-feature software for haplotype network construction. Methods Ecol. Evol. 6, 1110–1116. https://doi.org/10.1111/2041-210X.12410.

Lelong, A., Hégaret, H., Soudant, P., Bates, S.S., 2012. Pseudo-nitzschia (Bacillariophyceae) species, domoic acid and amnesic shellfish poisoning: revisiting previous paradigms. Phycologia 51, 168–216. https://doi.org/10.2216/11-37.1.

Ljubešić, Z., Bosak, S., Viličić, D., Borojević, K.K., Marić, D., Godrijan, J., Ujević, I., Peharec, P., Dakovac, T., 2011. Ecology and taxonomy of potentially toxic Pseudo-nitzschia species in Lim Bay (north-eastern Adriatic Sea). Harmful Algae 10, 713–722. https://doi.org/10.1016/j.hal.2011.06.002.

Lundholm, N., Moestrup, Ø., Hasle, G.R., Hoef-Emden, K., 2003. A study of the Pseudo-nitzschia pseudodelicatissima/cuspidata complex (Bacillariophyceae): What is P. pseudodelicatissima? J. Phycol. 39, 797–813. https://doi.org/10.1046/j.1529-8817.2003.02031.x.

Lundholm, N., Moestrup, Ø., Kotaki, Y., Hoef-Emden, K., Scholin, C., Miller, P., 2006. Inter- and intraspecific variation of the Pseudo-nitzschia delicatissima complex (Bacillariophyceae) illustrated by rRNA probes, morphological data and phylogenetic analyses. J. Phycol. 42, 464–481. https://doi.org/10.1111/j.1529-8817.2006.00211.x.

Lundholm, N., Bates, S.S., Baugh, K.A., Bill, B.D., Connell, L.B., Léger, C., Trainer, V.L., 2012. Cryptic and pseudo-cryptic diversity in diatoms-with descriptions of Pseudo-nitzschia hasleana sp. nov. and P. fryxelliana sp. nov. J. Phycol. 48, 436–454. https://doi.org/10.1111/j.1529-8817.2012.01132.x.

Luo, Z., Yang, W., Leaw, C.P., Pospelova, V., Bilien, G., Liow, G.R., Lim, P.T., Gu, H., 2017. Cryptic diversity within the harmful dinoflagellate Akashiwo sanguinea in coastal Chinese waters is related to differentiated ecological niches. Harmful Algae 66, 88–96. https://doi.org/10.1016/J.HAL.2017.05.008.

MacGillivary, M.L., Kaczmarska, I., 2011. Survey of the efficacy of a short fragment of the rbcL gene as a supplemental DNA barcode for diatoms. J. Eukaryot. Microbiol. 58, 529–536. https://doi.org/10.1111/j.1550-7408.2011.00585.x.

Malačič, V., 1991. Estimation of the vertical Eddy Diffusion-Coefficient of heat in the Gulf of Trieste (Northern Adriatic). Oceanol. Acta 14, 23–32.

Malačič, V., Celio, M., Čermelj, B., Bussani, A., Comici, C., 2006. Interannual evolution of seasonal thermohaline properties in the Gulf of Trieste (northern Adriatic) 1991-2003. J. Geophys. Res. Ocean 111. https://doi.org/10.1029/2005JC003267.

Marić, D., Ljubešić, Z., Godrijan, J., Viličić, D., Ujević, I., Precali, R., 2011. Blooms of the potentially toxic diatom Pseudo-nitzschia calliantha Lundholm, Moestrup & Hasle in coastal waters of the northern Adriatic Sea (Croatia). Estuar. Coast. Shelf Sci. 92, 323–331. https://doi.org/10.1016/j.ecss.2011.01.002.

Mccabe, R.M., Hickey, B.M., Kudela, R.M., Lefebvre, K.A., Adams, N.G., Bill, B.D., Gulland, F.M.D., Thomson, R.E., Cochlan, W.P., Trainer, V.L., 2016. An unprecedented coastwide toxic algal bloom linked to anomalous ocean conditions. Research Letter 366–376. https://doi.org/10.1002/2016GL070023.

Medlin, L.K., Orozco, J., 2017. Molecular techniques for the detection of organisms in aquatic environments, with emphasis on harmful algal bloom species. Sensors (Switzerland) 17. https://doi.org/10.3390/s17051184.

Mercado, J.M., Ramírez, T., Cortés, D., Sebastián, M., Vargas-Yáñez, M., 2005. Seasonal and inter-annual variability of the phytoplankton communities in an upwelling area of the Alborán Sea (SW Mediterranean Sea). Sci. Mar. 69, 451–465. https://doi.org/10.3989/scimar.2005.69n4451.

Moschandreou, K.K., Nikolaidis, G., 2010. The genus Pseudo-nitzschia (Bacillariophyceae) in Greek coastal waters. Bot. Mar. 53, 159–172. https://doi.org/10.1515/BOT.2010.014.

Moschandreou, K.K., Baxevanis, A.D., Katikou, P., Papaefthimiou, D., Nikolaidis, G., Abatzopoulos, T.J., 2012. Inter- and intra-specific diversity of Pseudo-nitzschia (Bacillariophyceae) in the northeastern Mediterranean. Eur. J. Phycol. 47, 321–339. https://doi.org/10.1080/09670262.2012.713998.

Mozetič, P., Fonda Umani, S., Cataletto, B., Malej, A., 1998. Seasonal and inter-annual plankton variability in the Gulf of Trieste (Northern Adriatic), in: ICES Journal of Marine Science. Narnia 711–722. https://doi.org/10.1006/jmsc.1998.0396.

Mozetič, P., Cangini, M., Francé, J., Bastianini, M., Bernardi Aubry, F., Bužančić, M., Cabrini, M., Cerino, F., Čalić, M., D'Adamo, R., Drakulović, D., Finotto, S., Fornasaro, D., Grilli, F., Kraus, R., Kužat, N., Marić Pfannkuchen, D., Ninčević Gladan, Ž., Pompei, M., Rotter, A., Servadei, I., Skejić, S., 2019. Phytoplankton diversity in

Adriatic ports: lessons from the port baseline survey for the management of harmful algal species. Mar. Pollut. Bull. https://doi.org/10.1016/j.marpolbul.2017.12.029.
Oksanen, J., Blanchet, F.G., Friendly, M., Kindt, R., Legendre, P., McGlinn, D., Minchin, P.R., O'Hara, R.B., Simpson, G.L., Solymos, P., Stevens, M.H.H., Szoecs, E., Wagner, H., 2019. Vegan: Community Ecology Package.
Orive, E., Laza-Martinez, A., Seoane, S., Alonso, A., Andrade, R., Miguel, I., 2010. Diversity of pseudo-nitzschia in the southeastern bay of biscay. Diatom Res. 25, 125–145. https://doi.org/10.1080/0269249X.2010.9705834.
Orive, E., Pérez-Aicua, L., David, H., García-Etxebarria, K., Laza-Martínez, A., Seoane, S., Miguel, I., 2013. The genus Pseudo-nitzschia (Bacillariophyceae) in a temperate estuary with description of two new species: Pseudo-nitzschia plurisecta sp. nov. and Pseudo-nitzschia abrensis sp. nov. J. Phycol. 49, 1192–1206. https://doi.org/10.1111/jpy.12130.
Orozco, J., Villa, E., Manes, C.L., Medlin, L.K., Guillebault, D., 2016. Electrochemical RNA genosensors for toxic algal species: enhancing selectivity and sensitivity. Talanta 161, 560–566. https://doi.org/10.1016/j.talanta.2016.08.073.
Orsini, L., Procaccini, G., Sarno, D., Montresor, M., 2004. Multiple rDNA ITS-types within the diatom Pseudo-nitzschia delicatissima (Bacillariophyceae) and their relative abundances across a spring bloom in the Gulf of Naples. Mar. Ecol. Prog. Ser. 271, 87–98. https://doi.org/10.3354/meps271087.
Patwardhan, A., Amit, R., Ray, S., 2014. Molecular markers in phylogenetic Studies-A review. J. Phylogenetics Evol. Biol. 2, 1–9. https://doi.org/10.4172/2329-9002.1000131.
Penna, A., Casabianca, S., Perini, F., Bastianini, M., Riccardi, E., Pigozzi, S., Scardi, M., 2013. Toxic Pseudo-nitzschia spp. In the northwestern Adriatic Sea: characterization of species composition by genetic and molecular quantitative analyses. J. Plankton Res. 35, 352–366. https://doi.org/10.1093/plankt/fbs093.
Pistocchi, R., Guerrini, F., Pezzolesi, L., Riccardi, M., Vanucci, S., Ciminiello, P., Dell'Aversano, C., Forino, M., Fattorusso, E., Tartaglione, L., Milandri, A., Pompei, M., Cangini, M., Pigozzi, S., Riccardi, E., 2012. Toxin levels and profiles in microalgae from the North-Western Adriatic Sea - 15 Years of studies on cultured species. Mar. Drugs. https://doi.org/10.3390/md10010140.
Posada, D., 2008. jModelTest: phylogenetic model averaging. Mol. Biol. Evol. 25, 1253–1256. https://doi.org/10.1093/molbev/msn083.
Potapova, M., Hamilton, P.B., 2007. Morphological and ecological variation within the Achnanthidium minutissimum (Bacillariophyceae) species complex. J. Phycol. 43, 561–575. https://doi.org/10.1111/j.1529-8817.2007.00332.x.
Pugliese, L., Casabianca, S., Perini, F., Andreoni, F., Penna, A., 2017. A high resolution melting method for the molecular identification of the potentially toxic diatom Pseudo-nitzschia spp. In the Mediterranean Sea. Sci. Rep. 7, 4259. https://doi.org/10.1038/s41598-017-04245-z.
Quijano-Scheggia, S., Garcés, E., Flo, E., Fernandez-Tejedor, M., Diogène, J., Camp, J., 2008a. Bloom dynamics of the genus Pseudo-nitzschia (Bacillariophyceae) in two coastal bays (NW Mediterranean Sea). Sci. Mar. 72, 577–590. https://doi.org/10.3989/scimar.2008.72n3577.
Quijano-Scheggia, S., Garcés, E., Sampedro, N., Van Lenning, K., Flo, E., Andree, K., Fortuño, J.M., Camp, J., 2008b. Identification and characterisation of the dominant Pseudo-nitzschia species (Bacillariophyceae) along the NE Spanish coast (Catalonia, NW Mediterranean). Sci. Mar. 72, 343–359. https://doi.org/10.3989/scimar.2008.72n2343.
Quijano-Scheggia, S.I., Garcés, E., Lundholm, N., Moestrup, Ø., Andree, K., Camp, J., 2009. Morphology, physiology, molecular phylogeny and sexual compatibility of the cryptic Pseudo-nitzschia delicatissima complex (Bacillariophyta), including the description of P. Arenysensis sp. Nov. Phycologia 48, 492–509. https://doi.org/10.2216/08-21.1.
R Core Team, 2019. R: A Language and Environment for Statistical Computing.
Rambaut, A., Drummond, A.J., Xie, D., Baele, G., Suchard, M.A., 2018. Posterior summarization in bayesian phylogenetics using tracer 1.7. Syst. Biol. (Stevenage) 67, 901–904. https://doi.org/10.1093/sysbio/syy032.
Ribera d'Alcalà, M., Conversano, F., Corato, F., Licandro, P., Mangoni, O., Marino, D., Mazzocchi, M.G., Modigh, M., Montresor, M., Nardella, M., Saggiomo, V., Sarno, D., Zingone, A., 2004. Seasonal patterns in plankton communities in a pluriannual time series at a coastal Mediterranean site (Gulf of Naples): an attempt to discern recurrences and trends. Sci. Mar. 68, 65–83. https://doi.org/10.3989/scimar.2004.68s165.
Richlen, M.L., Erdner, D.L., McCauley, L.A.R., Liberal, K., Anderson, D.M., 2012. Extensive genetic diversity and rapid population differentiation during blooms of alexandrium fundyense (Dinophyceae) in an isolated salt pond on cape cod, MA, USA. Ecol. Evol. 2, 2588–2599. https://doi.org/10.1002/ece3.373.
Rimet, F., Chaumeil, P., Keck, F., Kermarrec, L., Vasselon, V., Kahlert, M., Franc, A., Bouchez, A., 2016. R-Syst::Diatom: an Open-access and Curated Barcode Database for Diatoms and Freshwater Monitoring. Database 2016, baw016. https://doi.org/10.1093/database/baw016.
Ronquist, F., Teslenko, M., van der Mark, P., Ayres, D.L., Darling, A., Höhna, S., Larget, B., Liu, L., Suchard, M.A., Huelsenbeck, J.P., 2012. MrBayes 3.2: efficient Bayesian phylogenetic inference and model choice across a large model space. Syst. Biol. 61, 539–542. https://doi.org/10.1093/sysbio/sys029.
Ruggiero, M.V., Sarno, D., Barra, L., Kooistra, W.H.C.F., Montresor, M., Zingone, A., 2015. Diversity and temporal pattern of Pseudo-nitzschia species (Bacillariophyceae) through the molecular lens. Harmful Algae 42, 15–24. https://doi.org/10.1016/j.hal.2014.12.001.
Smith, M.W., Maier, M.A., Suciu, D., Peterson, T.D., Bradstreet, T., Nakayama, J., Simon, H.M., 2012. High resolution microarray assay for rapid taxonomic assessment of Pseudo-nitzschia spp. (Bacillariophyceae) in the field. Harmful Algae 19, 169–180. https://doi.org/10.1016/j.hal.2012.07.003.
Solidoro, C., Del Negro, P., Libralto, S., Malaku Canu, D., 2010. Sostenibilità Della Mitilicoltura Triestina. Istituto Nazionale di Oceanografia e di Geofisica Sperimentale-OGS.
Stern, R., Moore, S.K., Trainer, V.L., Bill, B.D., Fischer, A., Batten, S., 2018a. Spatial and temporal patterns of Pseudo-nitzschia genetic diversity in the North Pacific Ocean from the Continuous Plankton Recorder survey. Mar. Ecol. Prog. Ser. 606, 7–28. https://doi.org/10.3354/meps12711.
Stern, R., Kraberg, A., Bresnan, E., Kooistra, W.H.C.F., Lovejoy, C., Montresor, M., Morán, X.A.G., Not, F., Salas, R., Siano, R., Vaulot, D., Amaral-Zettler, L., Zingone, A., Metfies, K., 2018b. Molecular analyses of protists in long-term observation programmes - Current status and future perspectives. J. Plankton Res. 40, 519–536. https://doi.org/10.1093/plankt/fby035.
Talaber, I., Francé, J., Flander-Putrle, V., Mozetič, P., 2018. Primary production and community structure of coastal phytoplankton in the Adriatic Sea: insights on taxon-specific productivity. Mar. Ecol. Prog. Ser. 604, 65–81. https://doi.org/10.3354/meps12721.
Templeton, A.R., Crandall, K.A., Sing, C.F., 1992. A cladistic analysis of phenotypic associations with haplotypes inferred from restriction endonuclease mapping and DNA sequence data. III. Cladogram estimation. Genetics 132, 619–633.
Teng, S.T., Leaw, C.P., Lim, H.C., Lim, P.T., 2013. The genus Pseudo-nitzschia (Bacillariophyceae) in Malaysia, including new records and a key to species inferred from morphology-based phylogeny. Bot. Mar. 56, 375–398. https://doi.org/10.1515/bot-2012-0194.
Tesson, S.V.M., Montresor, M., Procaccini, G., Kooistra, W.H.C.F., 2014. Temporal changes in population structure of a marine planktonic diatom. PLoS One 9, 1–23. https://doi.org/10.1371/journal.pone.0114984.
Thorel, M., Claquin, P., Schapira, M., Le Gendre, R., Riou, P., Goux, D., Le Roy, B., Raimbault, V., Deton-Cabanillas, A.F., Bazin, P., Kientz-Bouchart, V., Fauchot, J., 2017. Nutrient ratios influence variability in Pseudo-nitzschia species diversity and particulate domoic acid production in the Bay of Seine (France). Harmful Algae 68, 192–205. https://doi.org/10.1016/j.hal.2017.07.005.
Throndsen, J., 1978. Preservation and storage. In: Sournia, A. (Ed.), Phytoplankton Manual. UNESCO, Paris, pp. 69–74.
Totti, C., Romagnoli, T., Accoroni, S., Coluccelli, A., Pellegrini, M., Campanelli, A., Grilli, F., Marini, M., 2019. Phytoplankton communities in the northwestern Adriatic Sea: interdecadal variability over a 30-years period (1988–2016) and relationships with meteoclimatic drivers. J. Mar. Syst. 193, 137–153. https://doi.org/10.1016/J.JMARSYS.2019.01.007.
Trainer, V.L., Hickey, B.M., Horner, R.A., 2002. Biological and physical dynamics of domoic acid production off the Washington coast. Limnol. Oceanogr. 47, 1438–1446. https://doi.org/10.4319/lo.2002.47.5.1438.
Trainer, V.L., Bates, S.S., Lundholm, N., Thessen, A.E., Cochlan, W.P., Adams, N.G., Trick, C.G., 2012. Pseudo-nitzschia physiological ecology, phylogeny, toxicity, monitoring and impacts on ecosystem health. Harmful Algae 14, 271–300. https://doi.org/10.1016/j.hal.2011.10.025.
Ujević, I., Ninčević-Gladan, Ž., Roje, R., Skejić, S., Arapov, J., Marasović, I., 2010. Domoic acid - a new toxin in the croatian adriatic shellfish toxin profile. Molecules 15, 6835–6849. https://doi.org/10.3390/molecules15106835.
Utermöhl, H., 1958. Zur Vervollkommnung der quantitativen phytoplankton-methodik. Sil Commun. 1953-1996 1953–1996 (9), 1–38. https://doi.org/10.1080/05384680.1958.11904091.
Vasselon, V., Rimet, F., Tapolczai, K., Bouchez, A., 2017. Assessing ecological status with diatoms DNA metabarcoding: scaling-up on a WFD monitoring network (Mayotte island, France). Ecol. Indic. 82, 1–12. https://doi.org/10.1016/j.ecolind.2017.06.024.
Viličić, D., Djakovac, T., Burić, Z., Bosak, S., 2009. Composition and annual cycle of phytoplankton assemblages in the northeastern Adriatic Sea. Bot. Mar. https://doi.org/10.1515/BOT.2009.004.
Zingone, A., Totti, C., Sarno, D., Cabrini, M., Caroppo, C., Giacobbe, M.G., Lugliè, A., Nuccio, C., Socal, G., 2010. Fitoplancton: metodiche di analisi quali-quantitativa. In: Socal, G., Buttino, I., Cabrini, M., Mangoni, O., Penna, A., Totti, C. (Eds.), Metodologie Di Studio Del Plancton Marino. Manuali E Linee Guida 56/2010. ISPRA SIBM, Rome, pp. 213–237.
Zingone, A., D'Alelio, D., Mazzocchi, M.G., Montresor, M., Sarno, D., Balestra, C., Cannavacciuolo, M., Casotti, R., Conversano, F., Di Capua, I., Iudicone, D., Margiotta, F., Passarelli, A., Percopo, I., Ribera d'Alcalà, M., Saggiomo, M., Saggiomo, V., Tramontano, F., Zazo, G., 2019. Time series and beyond: multifaceted plankton research at a marine Mediterranean LTER site. Nat. Conserv. 34, 273–310. https://doi.org/10.3897/natureconservation.34.30789.